Journal of Sound and Vibration (1999) **227**(4), 833–872
Article No. jsvi.1999.2388, available online at http://www.idealibrary.com on IDEAL®

DYNAMICS OF A ROTOR-BEARING SYSTEM EQUIPPED WITH A HYDRODYNAMIC THRUST BEARING

P. L. JIANG AND L. YU

Theory of Lubrication and Bearing Institute, Xi'an Jiaotong University, 710049, *Shaanxi, People's Republic of China*

(*Received* 24 *November* 1998, *and in final form* 12 *May* 1999)

The effect of a hydrodynamic thrust bearing on the dynamics of a rotor-bearing system is investigated systematically in this paper. The action of a thrust bearing is described as forces and moments in a static state and a series of dynamic coefficients in a dynamic state which are calculated from the *Reynolds* equation and its perturbed forms by using the boundary elements method. A lumped-mass model for system motion based on the *Myklestad* transfer matrix method is formulated considering the effects of thrust bearings and axial load. An interative procedure is proposed to sovle the indeterminate problem of load-sharing among journal bearings due to the introduction of thrust bearings. The effects of such parameters as stiffness of shaft, static loads of journal bearings, position of lumped mass, position of thrust bearing and arrangement of thrust bearings on the action of thrust bearings are discussed. The nature of this action reveals that thrust bearings not only provide stiffness and damping in a dynamic state, but also change the static deflection of the shaft, and thereby influence the static load-sharing of journal bearings. The present research helps to explain the variation of dynamic characteristics of a machine due to the introduction of thrust bearings, and also provide theoretical basis for the dynamic design considering the effect of thrust bearings.

1. INTRODUCTION

Rotordynamics has gone through stages such as characteristics of shaft (critical speed, unbalance response, etc.), rotordynamic characteristics of key parts or components (hydrodynamic journal bearings, seals, couplings, etc.), stability analysis, active and passive vibration control and non-linear dynamics, etc. [1–11]. The investigations have already advanced beyond the shaft itself. The components, which can show effects on characteristics of rotor systems, may be considered as study objects. Hydrodynamic bearings are regarded as the best sources of damping. A lot of interest has been paid to the rotordynamic characteristics of hydrodynamic journal bearings [12]. In contrast, the effect of thrust bearings has not been given adequate attention. In most cases, thrust bearings are treated as axial supports, and hence existing investigations are mostly concerned with their static characteristics and the axial motion of rotors [13–15]. Mittwollen *et al.* in 1991 [16] pointed out

0022-460X/99/440833 + 40 $30.00/0

the effect of hydrodynamic thrust bearings on the lateral vibration of rotor system. They defined a series of dynamic coefficients to describe the dynamic action of a hydrodynamic thrust bearing, and the effect of a thrust bearing on the lateral vibration of a single-mass rotor system was investigated thereafter. The effect was also shown by an experiment in their paper. But this effect has not yet been given the attention it deserves. In rotor systems, hydrodynamic thrust bearings as well as journal bearings are the only parts capable of being designed to control the vibrations of rotors, and therefore it is necessary to investigate this effect thoroughly and systematically.

There are many cases when thrust bearings greatly change the dynamic characteristics of rotating machinery in industrial practice [17]. But as this effect has not been studied sufficiently, when dynamic analysis and design of rotor systems are undertaken, attention is frequently paid to journal bearings, which have two consequences. On the one hand, inherent defects may be introduced into the system. As the action of thrust bearings is not sufficiently estimated, the drift of critical speeds caused by thrust bearings is certain to affect the normal operation of the machine. On the other hand, the action of thrust bearings to enhance stability and control vibration cannot have sufficient effect. Thrust bearings are frequently placed in positions where their actions are not strong. Their parameters such as oil-film thickness are chosen in order that it does not give full to this kind of effect. Consequently the effects of thrust bearings in many machine are not obvious.

In rotating machinery, the dynamic responses of the shaft depend to a large extent on damping provided by all sorts of hydrodynamic bearings including thrust bearings. Therefore, as a kind of damping source, thrust bearings must be treated with the importance accorded to journal bearings. Most rotating machines are equipped with double-facet thrust bearings to balance the axial loads. As the axial clearance between the runner and the collar can be adjusted conveniently, and the oil-supplying system can be designed along with that of journal bearings, the dynamic design of thrust bearings is expected to be a measure to enhance the stability of system.

The introduction of thrust bearings changes the boundary condition of a system, and therefore changes the static equilibrium state. Even for a single-mass rotor system supported by two journal bearings at both ends and a thrust bearing in the axial direction, the load-sharing between journal bearings becomes a static indeterminate problem, and therefore the static coupling must be considered.

It is pointed out by vibration theory that the axial force can influence the critical speeds of a shaft to some degree [18]. Therefore, the effect of the static force which thrust bearings balance on the lateral vibration must be accounted for.

In this paper, the effect of a hydrodynamic thrust bearing on the lateral vibration of a rotor-bearing system is investigated systematically. Effects such as influence of axial force on lateral vibration, offset-load effect in journal bearings and static coupling between the thrust bearing and the rotor system, etc., are considered. The nature of the effect of thrust bearings on rotor-bearing systems and the factors affecting this effect are discussed in detail.

2. ROTORDYNAMIC MODELLING OF A HYDRODYNAMIC THRUST BEARING

A hydrodynamic thrust bearing in operation is shown in Figure 1. The runner of the thrust bearing translates in the axial direction and rotates around the x- and y-axis, and therefore the thrust bearing provides five actions to the system, namely W_z, W_x, W_y, M_x^p and M_y^p, as shown in the figure, which are due to the normal pressure produced by the oil film. The thrust bearing is supposed to work under isothermal conditions. Accordingly, the normal pressure on the jth pad satisfies the following *Reynolds* equation:

$$\frac{\partial}{\partial x}\left(\frac{h^3}{12\mu}\frac{\partial p}{\partial x}\right)+\frac{\partial}{\partial y}\left(\frac{h^3}{12\mu}\frac{\partial p}{\partial y}\right)=\frac{\omega}{2}\frac{\partial h}{\partial \theta}+\frac{\partial h}{\partial t}. \tag{1}$$

Oil thickness h is not only a function of the pad parameters, but also that of the motional parameters of rotor φ and ψ. It can be written from Figure 2 as

$$h = h_p + \alpha_0 r\sin(\theta_p-\theta) - \psi_j r\cos\theta - \varphi_j r\sin\theta, \tag{2}$$

where

$$\begin{aligned}\varphi_j &= \varphi\cos\alpha_j - \psi\sin\alpha_j,\\ \psi_j &= \varphi\sin\alpha_j + \psi\cos\alpha_j.\end{aligned} \tag{3}$$

In local co-ordinate system, the load capacity of a single pad is

$$\mathbf{W}_0 = W_{x0}\mathbf{i} + W_{y0}\mathbf{j} + W_{z0}\mathbf{k}, \tag{4}$$

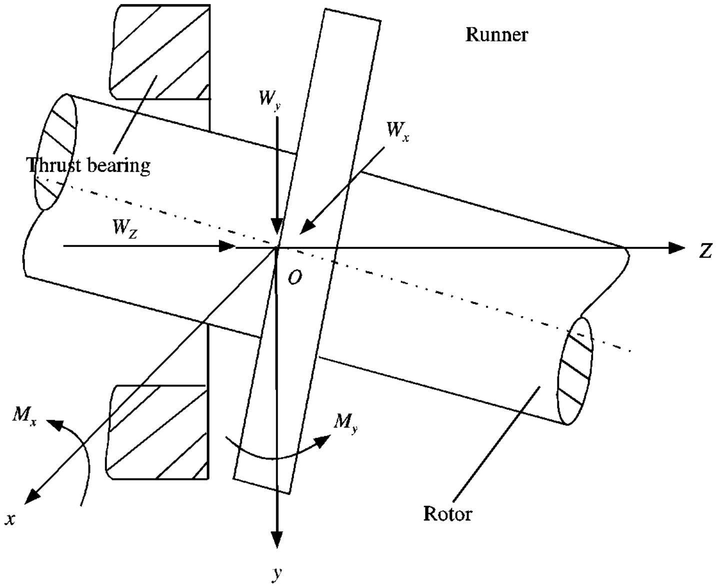

Figure 1. A hydrodynamic thrust bearing in operation.

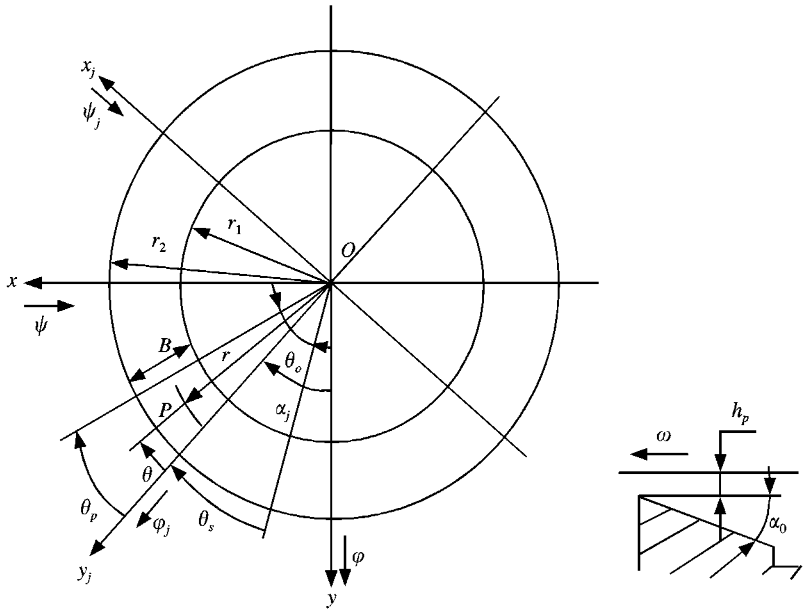

Figure 2. Parameters of thrust bearing.

with

$$\begin{Bmatrix} W_{x0} \\ W_{y0} \\ W_{z0} \end{Bmatrix} = W_0 \begin{Bmatrix} \sin\varphi_j \\ \cos\varphi_j \sin\psi_j \\ \cos\varphi_j \cos\psi_j \end{Bmatrix} \approx W_0 \begin{Bmatrix} \varphi_{j0} \\ \psi_{j0} \\ 1{\cdot}0 \end{Bmatrix},$$

$$W_0 = \iint\limits_{\Omega_j} p_0 r \,\mathrm{d}r\,\mathrm{d}\theta, \tag{5}$$

where Ω_j refers to the surface of the jth pad.

The moment vector due to normal oil-film pressure is

$$\mathbf{M}_0^p = M_{x0}^p \mathbf{i} + M_{y0}^p \mathbf{j} + M_{z0}^p \mathbf{k}, \tag{6}$$

with

$$\begin{Bmatrix} M_{x0}^p \\ M_{y0}^p \\ M_{z0}^p \end{Bmatrix} = \begin{Bmatrix} \iint\limits_{\Omega_j} p_0 r^2 \cos\theta \,\mathrm{d}r\,\mathrm{d}\theta \\ -\iint\limits_{\Omega_j} p_0 r^2 \sin\theta \,\mathrm{d}r\,\mathrm{d}\theta \\ -M_{x0}^p \varphi_{j0} - M_{y0}^p \psi_{j0} \end{Bmatrix}. \tag{7}$$

In the case of small perturbation, the increment of **W** can be expressed in the form of stiffness and damping coefficients, i.e.,

$$\Delta\mathbf{W} = \Delta W_x\mathbf{i} + \Delta W_y\mathbf{j} + \Delta W_z\mathbf{k}, \tag{8}$$

where

$$\begin{Bmatrix} \Delta W_x \\ \Delta W_y \\ \Delta W_z \end{Bmatrix}_j = \begin{Bmatrix} k_{xh}^W & k_{x\varphi}^W & k_{x\psi}^W \\ k_{yh}^W & k_{y\varphi}^W & k_{y\psi}^W \\ k_{zh}^W & k_{z\varphi}^W & k_{z\psi}^W \end{Bmatrix}_j \begin{Bmatrix} \Delta h_p \\ \Delta\varphi \\ \Delta\psi \end{Bmatrix}_j + \begin{Bmatrix} d_{xh}^W & d_{x\varphi}^W & d_{x\psi}^W \\ d_{yh}^W & d_{y\varphi}^W & d_{y\psi}^W \\ d_{zh}^W & d_{z\varphi}^W & d_{z\psi}^W \end{Bmatrix}_j \begin{Bmatrix} \dot{h}_p \\ \dot{\varphi} \\ \dot{\psi} \end{Bmatrix}_j, \tag{9}$$

k_{is}^W is the force stiffness coefficients in the i direction when the degree of freedom s is perturbed, and d_{is}^W is the force damping coefficients in the i direction when velocity $\dot{s}$ is perturbed ($i = x, y, z$; $s = h_p, \varphi_j, \psi$). The moment dynamic coefficients can also be defined in the same manner.

The formulae for these coefficients are given as

$$\begin{Bmatrix} k_{xh}^W \\ k_{x\varphi}^W \\ k_{x\psi}^W \end{Bmatrix} = \begin{Bmatrix} \varphi_0 k_{zh}^W \\ \varphi_0 k_{z\varphi}^W + W_0 \\ \varphi_0 k_{z\psi}^W \end{Bmatrix}, \begin{Bmatrix} d_{xh}^W \\ d_{x\varphi}^W \\ d_{x\psi}^W \end{Bmatrix} = \varphi_0 \begin{Bmatrix} d_{zh}^W \\ d_{z\varphi}^W \\ d_{z\psi}^W \end{Bmatrix},$$

$$\begin{Bmatrix} k_{yh}^W \\ k_{y\varphi}^W \\ k_{y\psi}^W \end{Bmatrix} = \begin{Bmatrix} \varphi_0 k_{zh}^W \\ \varphi_0 k_{z\varphi}^W \\ \varphi_0 k_{z\psi}^W + W_0 \end{Bmatrix}, \begin{Bmatrix} d_{yh}^W \\ d_{y\varphi}^W \\ d_{y\psi}^W \end{Bmatrix} = \varphi_0 \begin{Bmatrix} d_{sh}^W \\ d_{z\varphi}^W \\ d_{z\psi}^W \end{Bmatrix},$$

$$k_{zh}^W = \iint\limits_{\Omega_j} \frac{\partial p}{\partial h_p} r\,\mathrm{d}r\,\mathrm{d}\theta, \qquad d_{zh}^W = \iint\limits_{\Omega_j} \frac{\partial p}{\partial \dot{h}_p} r\,\mathrm{d}r\,\mathrm{d}\theta,$$

$$k_{z\varphi}^W = \iint\limits_{\Omega_j} \frac{\partial p}{\partial \varphi_j} r\,\mathrm{d}r\,\mathrm{d}\theta, \qquad d_{z\varphi}^W = \iint\limits_{\Omega_j} \frac{\partial p}{\partial \dot{\varphi}_j} r\,\mathrm{d}r\,\mathrm{d}\theta,$$

$$k_{z\psi}^W = \iint\limits_{\Omega_j} \frac{\partial p}{\partial \psi_j} r\,\mathrm{d}r\,\mathrm{d}\theta, \qquad d_{z\psi}^W = \iint\limits_{\Omega_j} \frac{\partial p}{\partial \dot{\psi}_j} r\,\mathrm{d}r\,\mathrm{d}\theta,$$

$$k_{xh}^M = \iint\limits_{\Omega_j} \frac{\partial p}{\partial h_p} r^2 \cos\theta\,\mathrm{d}r\,\mathrm{d}\theta, \qquad d_{xh}^M = \iint\limits_{\Omega_j} \frac{\partial p}{\partial \dot{h}_p} r^2 \cos\theta\,\mathrm{d}r\,\mathrm{d}\theta,$$

$$k_{x\varphi}^M = \iint\limits_{\Omega_j} \frac{\partial p}{\partial \varphi_j} r^2 \cos\theta\,\mathrm{d}r\,\mathrm{d}\theta, \qquad d_{x\varphi}^M = \iint\limits_{\Omega_j} \frac{\partial p}{\partial \dot{\varphi}_j} r^2 \cos\theta\,\mathrm{d}r\,\mathrm{d}\theta,$$

$$k^M_{x\psi} = \iint\limits_{\Omega_j} \frac{\partial p}{\partial \psi_j} r^2 \cos\theta \, \mathrm{d}r \, \mathrm{d}\theta, \qquad d^M_{x\psi} = \iint\limits_{\Omega_j} \frac{\partial p}{\partial \dot{\psi}_j} r^2 \cos\theta \, \mathrm{d}r \, \mathrm{d}\theta,$$

$$k^M_{yh} = \iint\limits_{\Omega_j} -\frac{\partial p}{\partial h_p} r^2 \sin\theta \, \mathrm{d}r \, \mathrm{d}\theta, \qquad d^M_{yh} = \iint\limits_{\Omega_j} -\frac{\partial p}{\partial \dot{h}_p} r^2 \sin\theta \, \mathrm{d}r \, \mathrm{d}\theta,$$

$$k^M_{y\varphi} = \iint\limits_{\Omega_j} -\frac{\partial p}{\partial \varphi_j} r^2 \sin\theta \, \mathrm{d}r \, \mathrm{d}\theta, \qquad d^M_{y\varphi} = \iint\limits_{\Omega_j} -\frac{\partial p}{\dot{\varphi}_j} r^2 \sin\theta \, \mathrm{d}r \, \mathrm{d}\theta,$$

$$k^M_{y\psi} = \iint\limits_{\Omega_j} -\frac{\partial p}{\partial \psi_j} r^2 \sin\theta \, \mathrm{d}r \, \mathrm{d}\theta, \qquad d^M_{y\psi} = \iint\limits_{\Omega_j} -\frac{\partial p}{\partial \dot{\psi}_j} r^2 \sin\theta \, \mathrm{d}r \, \mathrm{d}\theta. \quad (10)$$

The pressure and its partial derivatives in the above formulae are obtained from the *Reynolds* equation and its perturbed forms by using an iterative procedure based on the boundary element method. The details are omitted here.

In order to calculate the dynamic coefficients of forces and moments in a global co-ordinate system, the dynamic coefficients of a single pad are transformed into a global co-ordinate system. Therefore the dynamic coefficients in a global co-ordinate system are

$$\{W\}_j = [A_1]_j \{\tilde{W}\}_j, \quad \{M_j\} = [A_1]_j \{\tilde{M}\}_j, \quad \{K^W_z\}_j = [A_2]_j [\tilde{K}^W_z\}_j,$$

$$\{D^W_z\}_j = [A_2]_j \{\tilde{D}^W_z\}_j,$$

$$\{K^W_{xy}\}_j = [A_3]_j \{\tilde{K}^W_{xy}\}_j, \quad \{D^W_{xy}\}_j = [A_3]_j \{\tilde{D}^W_{xy}\}_j, \quad \{K^M_{xy}\}_j = [A_3]_j \{\tilde{K}^M_{xy}\}_j,$$

$$\{D^M_{xy}\}_j = [A_3]_j \{\tilde{D}^M_{xy}\}_j, \quad (11)$$

where

$$\{W\}_j = (W_{x0}, W_{y0}, W_{z0})^{\mathrm{T}}_j, \quad \{M\}_j = (M_{x0}, M_{y0}, M_{z0})^{\mathrm{T}}_j,$$

$$\{K^W_z\}_j = (k^W_{zh}, k^W_{z\varphi}, k^W_{z\psi})^{\mathrm{T}}_j, \quad \{D^W_z\}_j = (d^W_{zh}, d^W_{z\varphi}, d^W_{z\psi})^{\mathrm{T}}_j,$$

$$\{K^W_{xy}\}_j = (k^W_{xh}, k^W_{x\varphi}, k^W_{x\psi}, k^W_{yh}, k^W_{y\varphi}, k^W_{y\psi})^{\mathrm{T}}_j, \quad \{D^W_{xy}\}_j = (d^W_{xh}, d^W_{x\varphi}, d^W_{x\psi}, d^W_{yh}, d^W_{y\varphi}, d^W_{y\psi})^{\mathrm{T}}_j,$$

$$\{K^M_{xy}\}_j = (k^M_{xh}, k^M_{x\varphi}, k^M_{x\psi}, k^M_{yh}, k^M_{y\varphi}, k^M_{y\psi})^{\mathrm{T}}_j, \quad \{D^M_{xy}\}_j = (d^M_{xh}, d^M_{x\varphi}, d^M_{x\psi}, d^M_{yh}, d^M_{y\varphi}, d^M_{y\psi})^{\mathrm{T}}_j,$$

$$[A_1]_j = \begin{bmatrix} \cos\alpha_j & \sin\alpha_j & 0 \\ -\sin\alpha_j & \cos\alpha_j & 0 \\ 0 & 0 & 1 \end{bmatrix}, \qquad [A_2]_j = \begin{bmatrix} 1 & 0 & 0 \\ 0 & \cos\alpha_j & \sin\alpha_j \\ 0 & -\sin\alpha_j & \cos\alpha_j \end{bmatrix},$$

$$[A_3]_j =$$

$$\begin{bmatrix} \cos\alpha_j & 0 & 0 & \sin\alpha_j & 0 & 0 \\ 0 & \cos^2\alpha_j & \cos\alpha_k\sin\alpha_j & 0 & \cos\alpha_j\sin\alpha_j & \sin^2\alpha_j \\ 0 & -\cos\alpha_j\sin\alpha_j & \cos^2\alpha_j & 0 & -\sin^2\alpha_j & \cos\alpha_j\sin\alpha_j \\ -\sin\alpha_j & 0 & 0 & \cos\alpha_j & 0 & 0 \\ 0 & -\cos\alpha_j\sin\alpha_j & -\sin^2\alpha_j & 0 & \cos^2\alpha_j & \cos\alpha_j\sin\alpha_j \\ 0 & \sin^2\alpha_j & -\cos\alpha_j\sin\alpha_j & 0 & -\cos\alpha_j\sin\alpha_j & \cos^2\alpha_j \end{bmatrix}.$$

The dynamic coefficients of the thrust bearing can be obtained by summing up coefficients of all the pads in the global co-ordinate system.

3. FORMULATION OF THE SYSTEM EQUATIONS

The lumped-mass model, which can consider the deflection angles with ease, is used to formulate the system equations. A lumped-mass model considering the effect of axial force on lateral vibration of a shaft is presented in this paper. It is based on the *Myklestad* transfer matrix method, in which the shaft is discretized into several elements, and each element is simplified into a massless elastic rod and a lumped mass at the right end of the rod. When the relation among the adjacent elements is found, the motion equations for each element and the system are obtained accordingly.

For element j shown in Figure 3, the equilibrium equations considering the axial force can be written as

$$M_{j-1} + T_j(x_j - x_{j-1}) - S_{j-1} l_j = M_j + M_{kj}, \tag{12}$$

$$S_j = S_{j-1} + \sum P_{xj}, \tag{13}$$

$$x_j = x_{j-1} + \varphi_{j-1} l_j - T_j\varphi_j \frac{l_j^3}{3EI_j} + (M_j + M_{kj})\frac{l_j^2}{2EI_j} + \left(S_j - \sum P_{xj}\right)\frac{l_j^3}{3EI_j}, \tag{14}$$

$$\varphi_j = \varphi_{j-1} - T_j\varphi_j \frac{l_j^2}{2EI_j} + (M_j + M_{kj})\frac{l_j}{EI_j} + \left(S_j - \sum P_{xj}\right)\frac{l_j^2}{2EI_j}, \tag{15}$$

where $\sum P_x$ and M_k are respectively the external force and moment including the inertial force and bearing force, etc., S and M are respectively the force and moment exerted on the lumped mass by the rod, x and φ are respectively the displacement and angle.

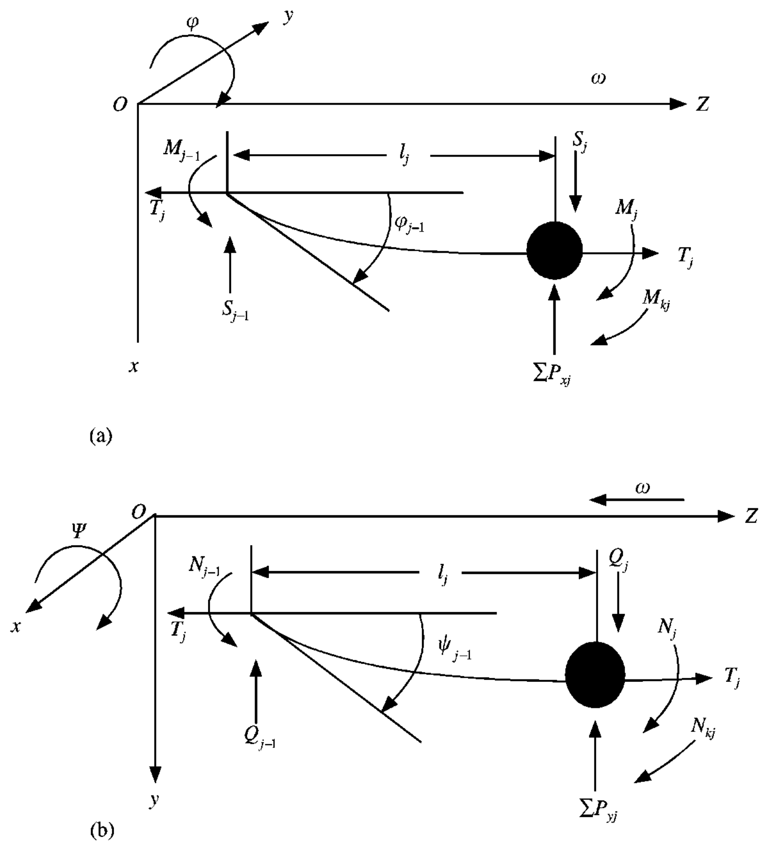

Figure 3. The jth shaft element.

For equation (15),

$$\varphi_{j-1} = \varphi_j\left(1 + T_j\frac{l_j^2}{2EI_j}\right) - (M_j + M_{kj})\frac{l_j}{EI_j} - \left(S_j - \sum P_{xj}\right)\frac{l_j^2}{2EI_j}. \tag{16}$$

From equations (14) and (16),

$$x_{j-1} = x_j - \varphi_j\left(l_j + T_j\frac{l_j^3}{6EI_j}\right) + (M_j + M_{kj})\frac{l_j^2}{2EI_j} + \left(S_j - \sum P_{xj}\right)\frac{l_j^3}{6EI_j}. \tag{17}$$

From equation (20),

$$M_{j-1} = (M_{kj} + M_j)(1 + T_j)\frac{l_j^2}{2EI_j} + \left(S_j - \sum P_{xj}\right)\left(l_j + \frac{T_j l_j^3}{6EI_j}\right) - T_j\varphi_j\left(l_j + \frac{T_j l_j^3}{6EI_j}\right). \tag{18}$$

Therefore,

$$\begin{Bmatrix} x \\ \varphi \\ M \\ S \end{Bmatrix}_{j-1} = \begin{bmatrix} 1 & -\left(l + \dfrac{Tl^3}{6EI}\right) & \dfrac{l^2}{2EI} & \dfrac{l^3}{6EI} \\ 0 & \left(1 + \dfrac{Tl^2}{2EI}\right) & -\dfrac{l}{EI} & -\dfrac{l^2}{2EI} \\ 0 & -T\left(l + \dfrac{Tl^3}{6EI}\right) & \left(1 + \dfrac{Tl^2}{2EI}\right) & \left(l + \dfrac{Tl^3}{6EI}\right) \\ 0 & 0 & 0 & 1 \end{bmatrix}_j \begin{Bmatrix} x \\ \varphi \\ (M + M_k) \\ (S - \sum P_x) \end{Bmatrix}_j . \tag{19}$$

Denote

$$\begin{Bmatrix} x \\ \varphi \\ M \\ S \end{Bmatrix}_j^R = [A]_j^{-1} \begin{Bmatrix} x \\ \varphi \\ M \\ S \end{Bmatrix}_{j-1}^R + \begin{Bmatrix} 0 \\ 0 \\ -M_k \\ \sum P_x \end{Bmatrix}_j^R , \tag{20}$$

$$[A]_j^{-1} = \begin{bmatrix} B & C \\ D & E \end{bmatrix}_j ,$$

where

$$[B]_j = \frac{1}{1 + \dfrac{T_j^2 l_j^4}{12(EI_j)^2}} \begin{bmatrix} \left[1 + \dfrac{T^2 l^4}{12(EI)^2}\right] & \left(l + \dfrac{Tl^3}{6EI}\right) \\ 0 & \left(1 + \dfrac{Tl^2}{2EI}\right) \end{bmatrix}_j ,$$

$$[D]_j = \frac{1}{1 + \dfrac{T_j^2 l_j^4}{12(EI_j)^2}} \begin{bmatrix} 0 & T\left(l + \dfrac{Tl^3}{6EI}\right) \\ 0 & 0 \end{bmatrix}_j$$

$$[C]_j = \frac{1}{1 + \dfrac{T_j^2 l_j^4}{12(EI_j)^2}} \begin{bmatrix} \dfrac{l^2}{2EI}\left(1 - \dfrac{Tl^2}{6EI}\right) & -\dfrac{l^3}{6EI}\left(1 - \dfrac{Tl^2}{2EI}\right) \\ \dfrac{l}{EI} & -\dfrac{l^2}{2EI}\left(1 - \dfrac{Tl^2}{6EI}\right) \end{bmatrix}_j ,$$

$$[E]_j = \frac{1}{1 + \dfrac{T_j^2 l_j^4}{12(EI_j)^2}} \begin{bmatrix} \left(1 + \dfrac{Tl^2}{2EI}\right) & -\left(l + \dfrac{Tl^3}{6EI}\right) \\ 0 & \left[1 + \dfrac{T^2 l^4}{12(EI)^2}\right] \end{bmatrix}.$$

From equation (20), the relation between the generalized forces exerted on the $(j-1)$th mass and the generalized displacements satisfies

$$\begin{Bmatrix} M \\ S \end{Bmatrix}_{j-1}^R = [C]_j^{-1} \begin{Bmatrix} x \\ \varphi \end{Bmatrix}_j^R - [C]_j^{-1} [B]_j \begin{Bmatrix} x \\ \varphi \end{Bmatrix}_{j-1}^R \tag{21}$$

therefore the equations for jth mass in the x direction are

$$- [C]_{j+1}^{-1} \begin{Bmatrix} x \\ \varphi \end{Bmatrix}_{j+1}^R + [C]_{j+1}^{-1} [B]_{j+1} \begin{Bmatrix} x \\ \varphi \end{Bmatrix}_j^R + \begin{Bmatrix} -M_k \\ \sum P_x \end{Bmatrix}_j^R + [D]_j \begin{Bmatrix} x \\ \varphi \end{Bmatrix}_{j-1}^R$$

$$+ [E]_j \left([C]_j^{-1} \begin{Bmatrix} x \\ \varphi \end{Bmatrix}_j^R - [C]_j^{-1} [B]_j \begin{Bmatrix} x \\ \varphi \end{Bmatrix}_{j-1}^R \right) = 0. \tag{22}$$

The inertial forces and moments and the forces and moments provided by the thrust bearing are

$$\begin{bmatrix} M_k \\ N_k \end{bmatrix} = \begin{bmatrix} -\theta_y & 0 \\ 0 & -\theta_x \end{bmatrix}_j \begin{Bmatrix} \ddot{\varphi} \\ \ddot{\psi} \end{Bmatrix}_j + \begin{bmatrix} 0 & \theta_z \omega \\ -\theta_z \omega & 0 \end{bmatrix}_j \begin{Bmatrix} \dot{\varphi} \\ \dot{\psi} \end{Bmatrix}_j + \begin{bmatrix} d_{y\varphi}^M & d_{y\psi}^M \\ -d_{x\varphi}^M & -d_{x\psi}^M \end{bmatrix}_j \begin{Bmatrix} \dot{\varphi} \\ \dot{\psi} \end{Bmatrix}_j$$

$$+ \begin{bmatrix} k_{y\varphi}^M & k_{y\psi}^M \\ -k_{x\varphi}^M & -k_{x\psi}^M \end{bmatrix}_j \begin{Bmatrix} x \\ y \end{Bmatrix}_j + \begin{bmatrix} k_{yh}^M \\ -k_{xh}^M \end{bmatrix} h_p + \begin{bmatrix} d_{yh}^M \\ -d_{xh}^M \end{bmatrix} \dot{h}_p, \tag{23}$$

$$\begin{bmatrix} \sum P_x \\ \sum P_y \end{bmatrix}_j = \begin{bmatrix} -m & 0 \\ 0 & -m \end{bmatrix}_j \begin{Bmatrix} \ddot{x} \\ \ddot{y} \end{Bmatrix}_j + \begin{bmatrix} d_{xx} & d_{xy} \\ d_{yx} & d_{yy} \end{bmatrix}_j \begin{Bmatrix} \dot{x} \\ \dot{y} \end{Bmatrix}_j + \begin{bmatrix} k_{xx} & k_{xy} \\ k_{yx} & k_{yy} \end{bmatrix}_j \begin{Bmatrix} x \\ y \end{Bmatrix}_j$$

$$+ \begin{bmatrix} d_{x\varphi}^W & d_{x\psi}^W \\ d_{y\varphi}^W & d_{y\psi}^W \end{bmatrix}_j \begin{Bmatrix} \dot{\varphi} \\ \dot{\psi} \end{Bmatrix}_j + \begin{bmatrix} k_{x\varphi}^W & k_{x\psi}^W \\ k_{y\varphi}^W & k_{y\psi}^W \end{bmatrix} \begin{Bmatrix} x \\ y \end{Bmatrix}_j + \begin{bmatrix} k_{xh}^W \\ k_{yh}^W \end{bmatrix} h_p + \begin{bmatrix} d_{xh}^W \\ d_{yh}^W \end{bmatrix} \dot{h}_p. \tag{24}$$

Substitution of the above matrices and forces and moments into equation (22) gives

$$\begin{bmatrix} m & 0 & 0 & 0 \\ 0 & m & 0 & 0 \\ 0 & 0 & \theta_y & 0 \\ 0 & 0 & 0 & \theta_x \end{bmatrix}_j \begin{Bmatrix} \ddot{x} \\ \ddot{y} \\ \ddot{\varphi} \\ \ddot{\psi} \end{Bmatrix}_j + \begin{bmatrix} d_{xx} & d_{xy} & -d^W_{x\varphi} & -d^W_{x\psi} \\ d_{yx} & d_{yy} & -d^W_{y\varphi} & -d^W_{y\psi} \\ 0 & 0 & -d^M_{y\varphi} & (-d^M_{y\psi} - \theta_z\omega) \\ 0 & 0 & (d^M_{x\varphi} + \theta_z\omega) & d^M_{x\psi} \end{bmatrix}_j \begin{Bmatrix} \dot{x} \\ \dot{y} \\ \dot{\varphi} \\ \dot{\psi} \end{Bmatrix}_j$$

$$+ \begin{bmatrix} k_{xx} & k_{xy} & -k^W_{x\varphi} & -k^W_{x\psi} \\ k_{yz} & k_{yy} & -k^W_{y\varphi} & -k^W_{y\psi} \\ 0 & 0 & -k^M_{y\varphi} & -k^M_{y\psi} \\ 0 & 0 & k^M_{x\varphi} & k^M_{x\psi} \end{bmatrix}_j \begin{Bmatrix} x \\ y \\ \varphi \\ \psi \end{Bmatrix}_j$$

$$- \begin{bmatrix} \frac{12EI}{l^3} & 0 & \left(-\frac{6EI}{l^2} + T\right) & 0 \\ 0 & \frac{12EI}{l^3} & 0 & \left(-\frac{6EI}{l^2} + T\right) \\ \left(\frac{6EI}{l^2} - T\right) & 0 & \left(-\frac{2EI}{l} + Tl\right) & 0 \\ 0 & \left(\frac{6EI}{l^2} - T\right) & 0 & \left(-\frac{2EI}{l} + Tl\right) \end{bmatrix}_{(j+1)} \begin{Bmatrix} x \\ y \\ \varphi \\ \psi \end{Bmatrix}_{(j+1)}$$

$$- \begin{bmatrix} \frac{12EI}{l^3} & 0 & \frac{6EI}{l^2} & 0 \\ 0 & \frac{12EI}{l^3} & 0 & \frac{6EI}{l^2} \\ -\frac{6EI}{l^2} & 0 & \left(-\frac{2EI}{l} + Tl\right) & 0 \\ 0 & -\frac{6EI}{l^2} & 0 & \left(-\frac{2EI}{l} + Tl\right)\Big/ cn \end{bmatrix}_j \begin{Bmatrix} x \\ y \\ \varphi \\ \psi \end{Bmatrix}_{(j-1)}$$

$$+ \begin{bmatrix} \frac{12EI}{l^3} & 0 & \frac{6EI}{l^2} & 0 \\ 0 & \frac{12EI}{l^3} & 0 & \frac{6EI}{l^2} \\ \left(\frac{6EI}{l^2} - T\right) & 0 & \frac{4EI}{l} + & 0 \\ 0 & \left(\frac{6EI}{l^2} - T\right) & 0 & \frac{4EI}{l} \end{bmatrix}_{(j+1)} \begin{Bmatrix} x \\ y \\ \varphi \\ \psi \end{Bmatrix}_j$$

$$
+\begin{bmatrix} \frac{12EI}{l^3} & 0 & \left(-\frac{6EI}{l^2}+T\right) & 0 \\ 0 & \frac{12EI}{l^3} & 0 & \left(-\frac{6EI}{l^2}+T\right) \\ -\frac{6EI}{l^2} & 0 & \frac{4EI}{l} & 0 \\ 0 & -\frac{6EI}{l^2} & 0 & \frac{4EI}{l} \end{bmatrix}_j \begin{Bmatrix} x \\ y \\ \varphi \\ \psi \end{Bmatrix}_j
$$

$$
+\begin{bmatrix} 0 & 0 & 0 & 0 \\ 0 & 0 & 0 & 0 \\ 0 & 0 & T\left(l+\frac{Tl^3}{6EI}\right)\Big/cn & 0 \\ 0 & 0 & 0 & T\left(l+\frac{Tl^3}{6EI}\right)\Big/cn \end{bmatrix}_j \begin{Bmatrix} x \\ y \\ \varphi \\ \psi \end{Bmatrix}_{(j-1)}
$$

$$
+\begin{bmatrix} -k_{xh}^W \\ -k_{yh}^W \\ -k_{yh}^M \\ k_{xh}^M \end{bmatrix} h_p + \begin{bmatrix} -d_{xh}^W \\ -d_{yh}^W \\ -d_{yh}^M \\ d_{xh}^M \end{bmatrix} \dot{h}_p = 0, \tag{25}
$$

where k_{ij} and d_{ij} $(i, j = x, y)$ are respectively the stiffness and damping coefficients of journal bearings, k_{ij}^M, d_{ij}^M, k_{ij}^W and d_{ij}^W $(i = x, y; j = \varphi, \psi)$ are respectively the stiffness and damping coefficients of the thrust bearing, $cn = 1 + (T_j^2 l_j^4/12(EI_j)^2)$.

For the first and last (nth) element, equation (22) is simplified into

$$
-[C\}_2^{-1}\begin{Bmatrix} x \\ \varphi \end{Bmatrix}_2 + [C]_2^{-1}[B]_2\begin{Bmatrix} x \\ \varphi \end{Bmatrix}_1 + \begin{Bmatrix} -M_k \\ \sum P_x \end{Bmatrix}_1 = 0, \tag{26}
$$

$$
\begin{Bmatrix} -M_k \\ \sum P_x \end{Bmatrix}_n + [D]_n\begin{Bmatrix} x \\ \varphi \end{Bmatrix}_{n-1} + [E]_n\left([C]_n^{-1}\begin{Bmatrix} x \\ \varphi \end{Bmatrix}_n - [C]_n^{-1}[B]_n\begin{Bmatrix} x \\ \varphi \end{Bmatrix}_{n-1}\right) = 0. \tag{27}
$$

The above two equations are the boundary conditions in the x direction. The equations in the y direction can also be obtained in a similar manner.

The equation for the axial motion is

$$
\sum m_j \ddot{h}_p - k_{zh}^W h_p - d_{zh}^W \dot{h}_p - k_{z\varphi}^W \varphi_j - k_{z\psi}^W \psi_j - d_{z\varphi}^W \dot{\varphi}_j - d_{z\psi}^W \dot{\psi}_j = 0. \tag{28}
$$

Assembly of the motion equations for all the elements gives the system equation in the matrix form

$$
[M]\{\ddot{X}\} + [C]\{\dot{X}\} + [K]\{X\} = 0, \tag{29}
$$

where $[M]$, $[C]$ and $[K]$ are the generalized mass, damping and stiffness matrices respectively, and $\{X\}$ is the vector for generalized displacements.

The above quadratic eigenvalue problem is solved by using the generalized inverse interation method proposed in reference [19]. The Gaussian elimination method is used to calculate the unbalance responses.

4. STATIC EQUILIBRIUM EQUATIONS

The dynamic coefficients of bearing, which must be determined before dynamic analysis, depend on the static working point of system. The involvement of thrust bearings makes the problem more complex. Let us take a single-mass rotor systems for example, which is supported by two journal bearings at both ends and a self-balancing double-facet thrust bearing in the axial direction. If the effect of thrust bearing is not considered, the load-sharing between the two journal bearings can be determined just by solving the force- and moment-balance equations. But when the thrust bearing is included, as the static boundary conditions are changed thereby, the Reynolds equations which determine the forces and moments of the thrust bearing and the journal bearings must be solved simultaneously with the above two balance equations. As the moments and forces are non-linear functions of the journal displacements or the runner displacement and tilting angles, an iterative procedure is inevitable.

The static equilibrium equations are obtained by substituting the following equations into equation (22):

$$
\begin{aligned}
M_k &= -\, M^p_{y0}, \\
\sum P_x &= F^j_{x0} - W_{x0}, \\
N_k &= M^p_{x0}, \\
\sum P_y &= F^j_{y0} - P_g - W_{y0},
\end{aligned} \tag{30}
$$

where M^p_{y0} and M^p_{x0} represent the moments on the xz and yz planes at the jth mass respectively, W_{x0} and W_{y0} represents the force in the x and y directions respectively, and F^j_{x0} and F^j_{y0} are respectively the forces produced by the journal bearings in the x and y directions, and P_g is the weight of lumped mass.

When the equations for all the elements are obtained, and all the static forces and moments are substituted into the above equations, the static equilibrium equations in matrix form are

$$[S]\{X\} = \{F\} - \{P^j\}, \tag{31}$$

where $[S]$ is the stiffness matrix of shaft, $\{F\}$ is the vector for generalized forces including the forces and moments produced by the thrust bearing, and $\{P^j\}$ is the vector of oil-film forces produced by the journal bearings.

Consider the balance in the axial direction

$$W_{z0} + F_{th} = 0, \tag{32}$$

where W_{z0} represents the oil-film force in the axial direction produced by the thrust bearings, F_{th} is the external force exerted in the axial direction.

Denoting the translational displacements where the journal bearings act as $\{x_2\}$, the other translational displacements and all the angular displacements as $\{x_1\}$, the generalized forces corresponding to $\{x\}_1, \{x_2\}$ are $\{F_1\}, \{F_2\}$ respectively, and equation (31) is rewritten as

$$\begin{bmatrix} S_{11} & S_{12} \\ S_{21} & S_{22} \end{bmatrix} \begin{Bmatrix} x_1 \\ x_2 \end{Bmatrix} = \begin{Bmatrix} F_1 \\ F_2 \end{Bmatrix} - \begin{Bmatrix} 0 \\ P^j \end{Bmatrix}, \tag{33}$$

where $\{F_1\}, \{F_2\}$ and $\{x_2\}$ are known, i.e., all the forces and the static positions of the journals except the oil-form forces produced by journal bearings are known. $\{x_1\}$ and $\{P^j\}$ can be obtained from the following equations:

$$\begin{Bmatrix} x_1 \\ P^j \end{Bmatrix} = \begin{bmatrix} S_{11}^{-1} & -S_{11}^{-1}S_{12} \\ -S_{21}S_{11}^{-1} & -S_{22} + S_{21}S_{11}^{-1}S_{12} \end{bmatrix} \begin{Bmatrix} F_1 \\ x_2 \end{Bmatrix} + \begin{Bmatrix} 0 \\ F_2 \end{Bmatrix}. \tag{34}$$

Let

$$\begin{bmatrix} S_{11}^{-1} & -S_{11}^{-1}S_{12} \\ -S_{21}S_{11}^{-1} & -S_{22} + S_{21}S_{11}^{-1}S_{12} \end{bmatrix} = \begin{bmatrix} b_{11} & b_{12} \\ b_{21} & b_{22} \end{bmatrix};$$

the iterative procedure is given below. The increments of variables in each step satisfy the following formulae:

$$\begin{Bmatrix} \Delta x_1 \\ \Delta P^j \end{Bmatrix}^{(k)} + \begin{Bmatrix} x_1 \\ P^j \end{Bmatrix}^{(k)} = \begin{bmatrix} b_{11} & b_{12} \\ b_{21} & b_{22} \end{bmatrix} \left(\begin{Bmatrix} F_1 \\ x_2 \end{Bmatrix}^{(k)} + \begin{Bmatrix} \Delta F_1 \\ \Delta x_2 \end{Bmatrix}^{(k)} \right) + \begin{Bmatrix} 0 \\ F_2 \end{Bmatrix}^{(k)} + \begin{Bmatrix} 0 \\ \Delta F_2 \end{Bmatrix}^{(k)}, \tag{35}$$

$$W_{z0}^{(k)} + \Delta W_{z0}^{(k)} + F_{th} = 0. \tag{36}$$

The rotordynamic coefficients are used to obtain the first order approximation of $\{\Delta F_1\}$,$\{\Delta F_2\}$, $\{\Delta P^j\}$ and ΔW_{z0}. When the displacements $\{x_1\}, \{x_2\}$ and z are increased by $\{\Delta x_1\}, \{\Delta x_2\}$ and Δz respectively, the increments of the generalized force are

$$\begin{Bmatrix} \Delta F_1 \\ \Delta F_2 \\ \Delta P_j \\ \Delta W_{z0} \end{Bmatrix} = \begin{bmatrix} S_\varphi^1 & 0 & S_h^1 \\ S_\varphi^2 & 0 & S_h^2 \\ 0 & S_j & 0 \\ S_{z\varphi}^1 & 0 & S_{zh} \end{bmatrix} \begin{Bmatrix} \Delta x_1 \\ \Delta x_2 \\ \Delta h_p \end{Bmatrix}, \tag{37}$$

where $\{S_{\varphi}^{1}\}$, $\{S_{\varphi}^{2}\}$, S_h^1, S_h^2, $\{S_{z\varphi}^{1}\}$ and S_{zh} are composed of the stiffness coefficients of the thrust bearing, k_{is}^{W} and k_{is}^{M} ($i = x, y, z; s = \varphi, \psi, h_p$); $\{S_j\}$ consists of the stiffness coefficients of the journal bearings, k_{ij} ($i, j = x, y$).

Substitution of equation (37) into equations (35) and (36) gives

$$\begin{Bmatrix} \Delta x_1 \\ S_j \Delta x_2 \end{Bmatrix}^{(k)} + \begin{Bmatrix} x_1 \\ P^j \end{Bmatrix}^{(k)} = \begin{bmatrix} b_{11} & b_{12} \\ b_{21} & b_{22} \end{bmatrix} \left(\begin{Bmatrix} F_1 \\ x_2 \end{Bmatrix}^{(k)} + \begin{Bmatrix} S_{\varphi 1} \Delta x_1 + S_h^1 \Delta h_p \\ \Delta x_2 \end{Bmatrix}^{(k)} \right) + \begin{Bmatrix} 0 \\ F_2 \end{Bmatrix}^{(k)}$$

$$+ \begin{Bmatrix} 0 \\ S_{\varphi 2} \Delta x_1 + S_h^2 \Delta h_p \end{Bmatrix}^{(k)}, \tag{38}$$

$$W_{z0}^{(k)} + S_{z\varphi}^{1(k)} \Delta x_1^{(k)} + S_{zh}^{(k)} \Delta h_p^{(k)} + F_{th} = 0. \tag{39}$$

Therefore, the increments in the kth step can be obtained from the following equation:

$$\begin{bmatrix} b_{11} S_{\varphi}^{1} & -b_{12} & -b_{11} S_h^1 \\ -b_{21} S_{\varphi}^{1} - S_{\varphi}^{2} & S_j - b_{22} & -S_h^2 \\ S_{z\varphi}^{1} & 0 & S_{zh} \end{bmatrix}^{(k)} \begin{Bmatrix} \Delta x_1 \\ \Delta x_2 \\ \Delta h_p \end{Bmatrix} = \begin{bmatrix} b_{11} & b_{12} \\ b_{21} & b_{22} \\ 0 & 0 \end{bmatrix}^{(k)} \begin{Bmatrix} F_1 \\ F_2 \end{Bmatrix}^{(k)}$$

$$+ \begin{Bmatrix} 0 \\ F_2 \\ 0 \end{Bmatrix}^{(k)} - \begin{Bmatrix} x_1 \\ P_j \\ (W_{z0} + F_{th}) \end{Bmatrix}^{(k)}. \tag{40}$$

The load sharing when the rotor is simply supported is determined initially to provide the initial values of the journal positions and forces. The axial force-balance equation is solved solely to give the initial value of the film thickness of the pitch line of the thrust bearing. As the stiffness coefficients are directly used to obtain the first-order approximation of the changes of static forces, this iteration converges very fast.

Because the static tilting angles of the runner on the xz and yz planes can result in static forces and moments in both the x and y directions, the journal bearings must bear the load in the x direction in addition, i.e., the offset-load effect occurs on the journal bearings. Since, the loads are not applied vertically to the journal bearings, and the forces and moments by the journal bearings are variable in the above iteration, the static and dynamic characteristics of journal bearings must be recalculated according to the magnitude and direction of the resultant force, except for 360° cylindrical bearing whose characteristics can be obtained directly through co-ordinate transform. The offset-load effect is considered in this paper.

5. EFFECT OF A THRUST BEARING ON THE STATICS AND DYNAMICS OF A ROTOR-BEARING SYSTEM

In order to reveal the nature of the action of thrust bearings on rotor-bearing, a numerical example is used to investigate the influence of a thrust bearing on a single-mass rotor-bearing system as shown in Figure 4.

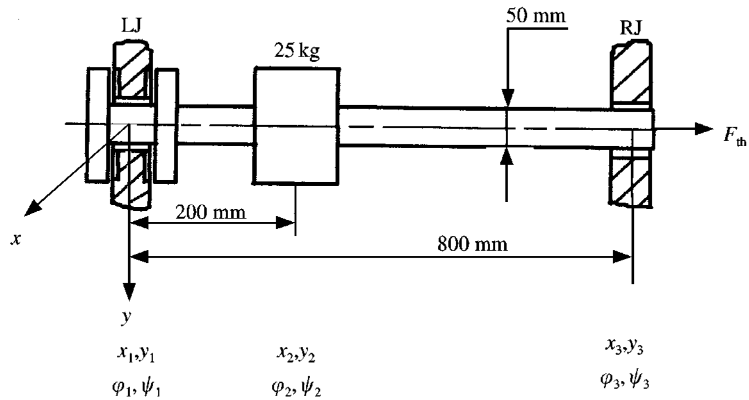

Figure 4. A rotor-bearing system with a hydrodynamic thrust bearing.

The rotor is supported by two identical 360° cylindrical journal bearings at both ends. A double-facet fixed-pad thrust bearing is attached at the left end, and is integrated with the left journal bearing to form a combined bearing. The parameters of the journal bearing are: diameter $D_0 = 50$ mm; ratio of length to diameter $L/D_0 = 0{\cdot}5$; clearance ratio $\Psi = 0{\cdot}001$. The parameters of the thrust bearings are: width of pad $B = 50$ mm; film thickness on pitch line $h_p = 0{\cdot}05$ mm; angular extent of pad $\theta_0 = 40°$; angular position of pitch line $\theta_p = \theta_0/2$; inner radius $r_1 = 50$ mm; wedge angle of pad $a_0 = 0{\cdot}02$ rad.

The dimensionless oil-film thickness is defined as $\bar{h} = h/h_e$ and the reference film thickness $h_e = 0{\cdot}05$ mm. The dynamic viscosity of oil $\mu = 0{\cdot}027$ N s/m^2 and the axial load $F_{th} = 0{\cdot}0$. The moments of inertia of the disk are assumed to be zero.

The thrust bearing and journal bearings are assumed to work under isothermal laminar conditions. The static and dynamic characteristics of journal bearings are calculated based on the short-bearing model.

5.1. INFLUENCE ON STATICS

Table 1 gives the displacements and angles at both ends of the disk. When the effect of the thrust bearing is not taken into account, there are no relative deflection angles among the elements on the *xz* plane, and the relative deflection angles on the *yz* plane are constant. This results from the fact that the journal bearings provide forces only, and the deflection angles are solely due to the distribution of weight. Although the oil-film forces of journal bearings are functions of rotating speed, the rotating speed only influences the journal positions. The static deflection of shaft is changed by the static moments of thrust bearing, and therefore the relative deflection angles among elements on the *yz* plane vary with rotating speed. The offset-load effect in journal bearings due to the thrust bearing leads to the relative deflection angles which vary with the rotating speed. From the table, when the rotating speed is 3000 r/min and the thrust bearing is included, the displacement at

TABLE 1

Static deflection of shaft

N (r/min)	Thrust bearing	x_1/D_0	x_2/D_0	x_3/D_0	φ_1	φ_2	φ_3
3000	NT	0·28875E − 4	0·25278E − 4	0·14486E − 4	−0·89935E − 6	− 0·89935E − 6	− 0·89935E − 6
9000	NT	0·90538E − 5	0·74689E − 5	0·27143E − 5	− 0·39622E − 6	− 0·39622E − 6	− 0·39622E − 6
3000	T	0·34287E − 4	0·36576E − 4	0·79600E − 5	0·17336E − 5	− 0·48391E − 6	− 0·33350E − 5
9000	T	0·11574E − 4	0·12376E − 4	0·10169E − 5	0·65135E − 6	− 0·20909E − 6	− 0·13154E − 5
N (r/min)	Thrust bearing	y_1/D_0	y_2/D_0	y_3/D_0	ψ_1	ψ_2	ψ_3
3000	NT	0·21326E − 5	0·58148E − 3	0·53488E − 6	0·16899E − 3	0·96524E − 4	− 0·12088E − 3
9000	NT	0·35487E − 5	0·58341E − 3	0·40048E − 5	0·16912E − 3	0·96653E − 4	− 0·12075E − 3
3000	T	0·31323E − 5	0·16648E − 3	0·39672E − 5	0·10438E − 4	0·42121E − 4	− 0·41375E − 4
9000	T	0·15633E − 5	0·14704E − 3	0·26984E − 5	0·36212E − 5	0·39790E − 4	− 0·37938E − 4

*NT—considering the effect of thrust bearing; T—not considering the effect of thrust bearing.

TABLE 2

Static characteristics of journal bearings

N (r/min)	LJ/RJ	Thrust bearing	ε	Dimensionless load capacity $\bar{W}$	Altitude angle θ	Load offset angle θ_W	x/D_0	y/D_0
3000	LJ	NT	0·57908E − 1	0·45883E − 1	0·14871E + 1	− 0·90555E − 8	0·28875E − 4	0·21326E − 5
9000	LJ	NT	0·19449E − 1	0·15295E − 1	0·11972E + 1	− 0·27952E − 8	0·90538E − 5	0·35487E − 5
3000	RJ	NT	0·28991E − 1	0·22827E − 1	0·15339E + 1	− 0·10488E − 8	0·14486E − 4	0·53488E − 6
9000	RJ	NT	0·96760E − 2	0·68483E − 2	0·59564E + 0	− 0·37315E − 9	0·27143E − 5	0·40048E − 5
3000	LJ	T	0·68860E − 1	0·54724E − 1	0·14831E + 1	− 0·34396E − 2	0·34287E − 4	0·31323E − 5
9000	LJ	T	0·23357E − 1	0·18368E − 1	0·14379E + 1	− 0·13254E − 2	0·11574E − 4	0·15633E − 5
3000	RJ	T	0·17788E − 1	0·13988E − 1	0·10950E + 1	0·13456E − 1	0·79600E − 5	0·39672E − 5
9000	RJ	T	0·57674E − 2	0·45355E − 2	0·35503E + 0	0·53678E − 2	0·10169E − 5	0·26984E − 5

LJ—left journal bearing; RJ—right journal bearing.

the disk in the y direction decreases by 71%, and the deflection at this point on the yz plane decreases by 97%.

Table 2 gives the variations of the working parameters of journal bearings due to the thrust bearing. The attitude angles and eccentricities change greatly when the thrust bearing is included. As the static moments of thrust bearing make the left journal go up and the right journal down, the eccentricity of the left journal bearing increases while that of the right decreases.

Figure 5 shows the variations of journal positions due to the thrust bearing. Figure 6 gives the variation of the dynamic coefficients of journal bearings versus the rotating speed. When the rotating speed is 3000 r/min, the thrust bearing makes

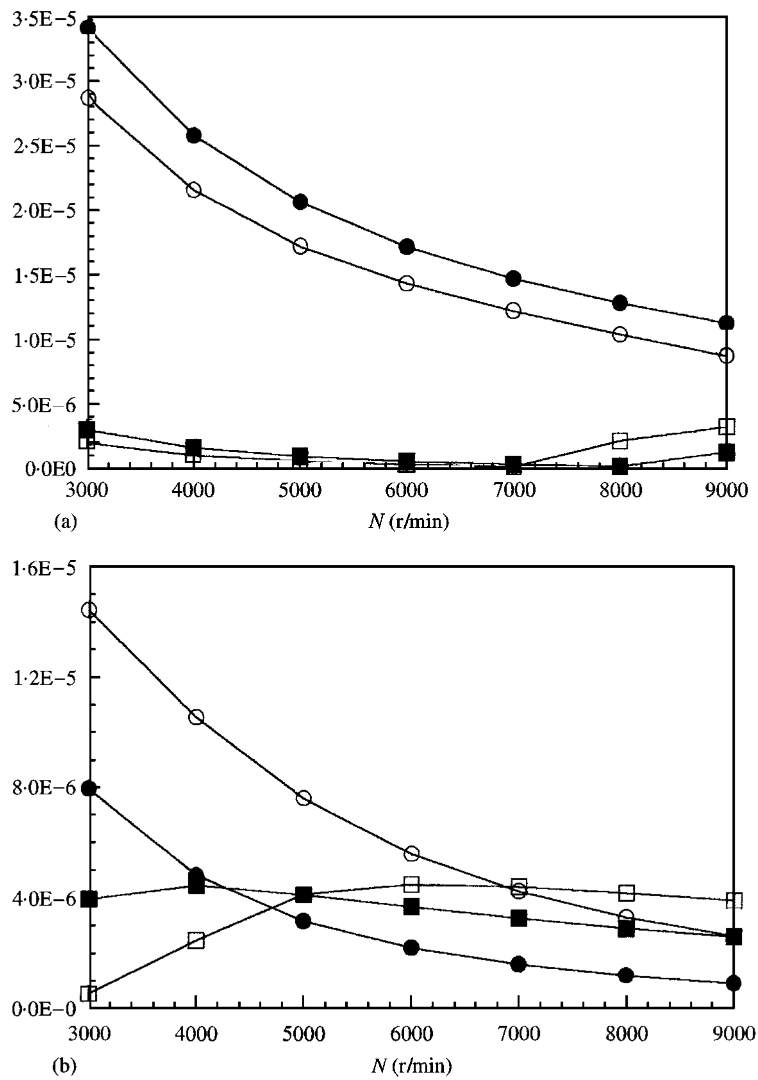

Figure 5. Variations of journal positions of both journal bearings versus rotating speed. (a) left journal bearing; (b) right journal bearing —○— x/D_0 NT, —□— y/D_0 NT, —●— x/D_0 T and —■— y/D_0 T.

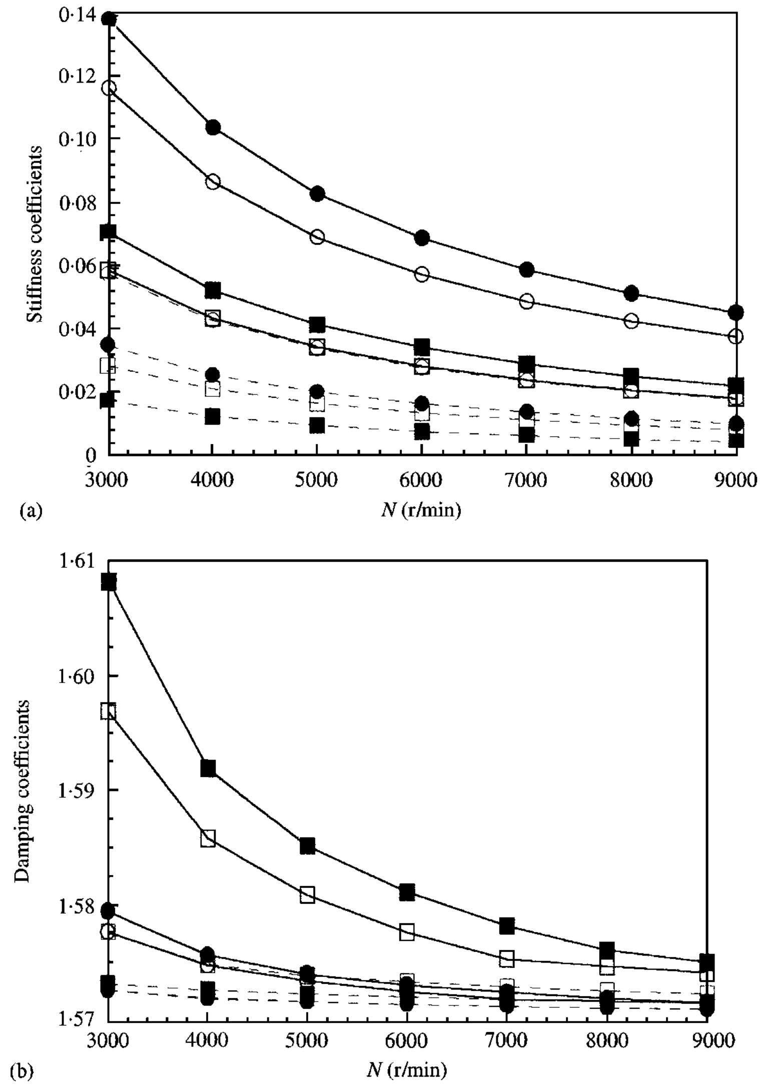

Figure 6. Variations of dynamics coefficients of both journal bearings versus rotating speed. (a) —○— $\bar{k}_{xx}$ LJ, NT; -○- - $\bar{k}_{xx}$ RJ, NT; —□— $\bar{k}_{yy}$ LJ, NT; -□- - $\bar{k}_{yy}$ RJ, NT; —●— $\bar{k}_{xx}$ LJ, T; -●- - $\bar{k}_{xx}$ RJ, T; —■— $\bar{k}_{yy}$ LJ, T; -■- - $\bar{k}_{yy}$ RJ, T; (b) —○— $\bar{d}_{xx}$ LJ, NT; -○- - $\bar{b}_{xx}$ RJ, NT; —□— $\bar{d}_{yy}$ LJ, NT; -□- - $\bar{d}_{yy}$ RJ, NT; —●— $\bar{d}_{xx}$ LJ, T; -●- - $\bar{d}_{xx}$ RJ, T; —■— $\bar{d}_{yy}$ LJ, T; -●- - $\bar{d}_{yy}$ RJ, T.

the direct stiffness of the left journal bearing increased by 20% and that of right decrease by 40%.

5.2. INFLUENCE ON DYNAMICS

The eigenvalues of the system at various rotating speeds can be obtained by solving equation (29), and the first critical speed and the stability threshold speed are calculated from these eigenvalues by interpolation. The numerical results show that when the thrust bearing is not considered, the first critical speed $N_{cr} = 5545$ r/min, while when the thrust bearing is considered, $N^*_{cr} = 11\,143$ r/min and is 2·01 times that of N_{cr}. The thrust bearing increases the first critical speed remarkably. The first simply supported critical speed of the shaft is 5533 r/min. When the thrust bearing is included, the critical speeds may exceed the simply supported critical speed. But for a rotor supported by journal bearings only, the critical speeds cannot exceed the simply supported critical speeds. Since the simple supports only restrians the displacements at both ends, while the thrust bearing influences the shaft stiffness at the deflection angles in addition, the simply supported case is the limit for a shaft supported solely by journal bearings.

Table 3 shows the variations of the real part of the first dimensionless eigenvalue versus the rotating speed. When the rotor is supported solely by journal bearings, the stability threshold speed of system is 9367 r/min. When the thrust bearing is included, it becomes 13511 r/min. The thrust bearing increases the stability threshold speed by 44%.

Figure 7 shows the variations of the unbalance responses versus the rotating speed. The offset of unbalance is supposed to be 0·025 mm and at the disk. The vibration magnitudes refer to those at the disk. It can be seen from the figure that the thrust bearing suppresses the unbalance responses at all the speeds significantly.

The nature of the thrust bearing action can be concluded from the above two sections. On the one hand, the static forces and moments of the thrust bearing changes the static equilibrium state of the shaft, and thereby change the load-sharing among journal bearings and their dynamic coefficients. On the other hand the stiffness and damping of thrust bearing influence the dynamic of the rotor directly. The effect of thrust bearing is the resultant action of both statics and dynamics.

6. FACTORS AFFECTING THE EFFECT OF THRUST BEARING

6.1. FILM THICKNESS OF THRUST BEARING AND AXIAL LOAD

It has been cited that the clearance between pad and collar can be adjusted conveniently. The film thickness is often designed according to the need of static characteristics, and the need of dynamic characteristics is seldom considered. Therefore, the discussion on the variation of film thickness is of great importance in the investigation into the action of thrust bearings. The rotor-bearing system shown in Figure 8 is studied. The parameter of the rotor are given in the figure, and those of the bearings are similar to those used in section 5. The dimensionless film thickness of the pitch line is changed continuously and the variations of static and dynamic characteristics of the system are observed. Figure 9 gives the deflection angles at both ends when the rotating speed is 3000 r/min. There are two limits for the static deflection angles corresponding to large and small film thickness respectively. When $\bar{h}_p$ is very large, i.e., at the lower limit, φ_1, φ_2 are zero, and ψ_1, ψ_2 are equal, which resembles the case when there is no thrust bearing acting on the system. When $\bar{h}_p$ is very small, i.e., at the upper limit, the action of thrust bearing,

TABLE 3

Variations of the real part of the first eigenvalue versus rotating speed

N (r/min)	4000	5000	6000	7000	8000	9000	10000	11000	12000	13000	14000
NT	−0·020	−0·016	−0·013	−0·010	−0·0077	−0·0031	0·0080	—	—	—	—
T	−0·013	−0·010	−0·0081	−0·0067	−0·0056	−0·0047	−0·0039	−0·0032	−0·0024	−0·0011	0·0013

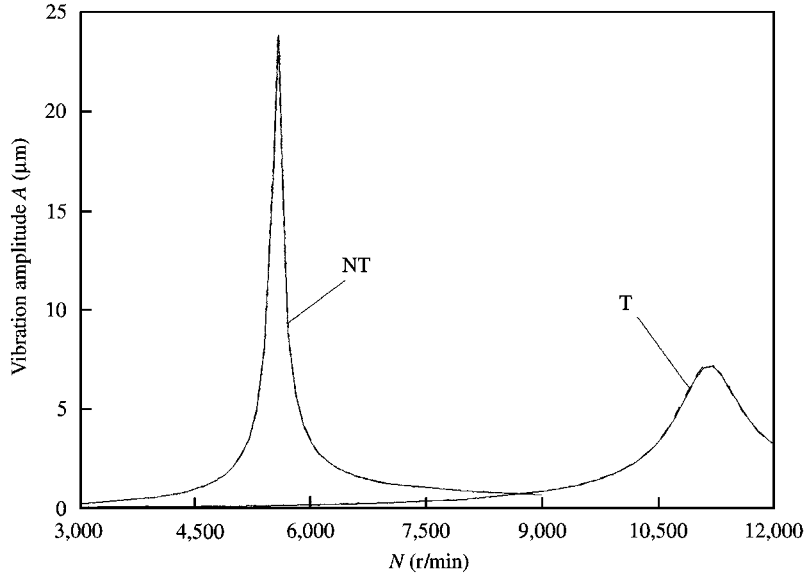

Figure 7. Unbalance response of the rotor. —— x; ---- y.

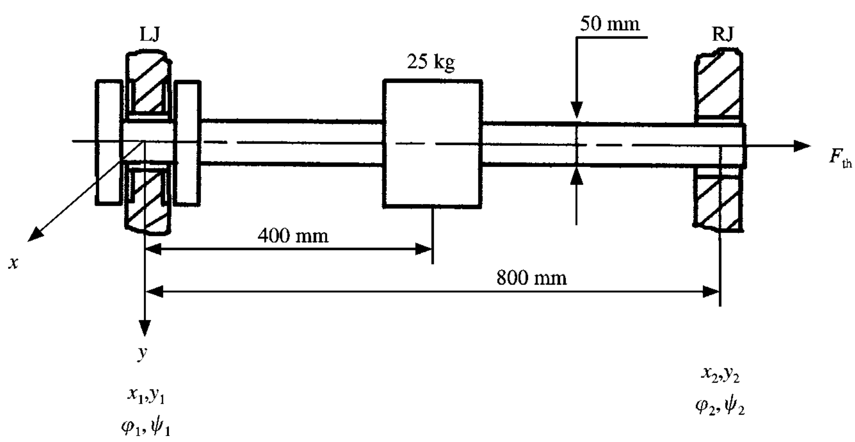

Figure 8. A rotor-bearing system with a hydrodynamic thrust bearing.

which hinders the deflection of the shaft, is so large that the offset-load in journal bearings vanishes, and φ_1, φ_2 and ψ_1 tend to zero.

Figure 10 shows the variations of the first critical speed ratio, N_{cr}^*/N_{cr}, and the stability threshold speed ratio, N_{st}^*/N_{st}, versus the dimensionless film thickness. The asterisk denotes the case when there is no thrust bearing included. There are two limits for the variations likewise. At the lower limit, N_{cr}^*/N_{cr} and N_{st}^*/N_{st} tend to 1, which indicates that the effect of thrust bearing is so small that it can be neglected. At the upper limit, N_{cr}^*/N_{cr} and N_{st}^*/N_{st} tend to specific values respectively, which means that the action of thrust bearing will not strengthen. Generally speaking, the thrust bearing always hinders the deflection of the shaft, and hence at the upper

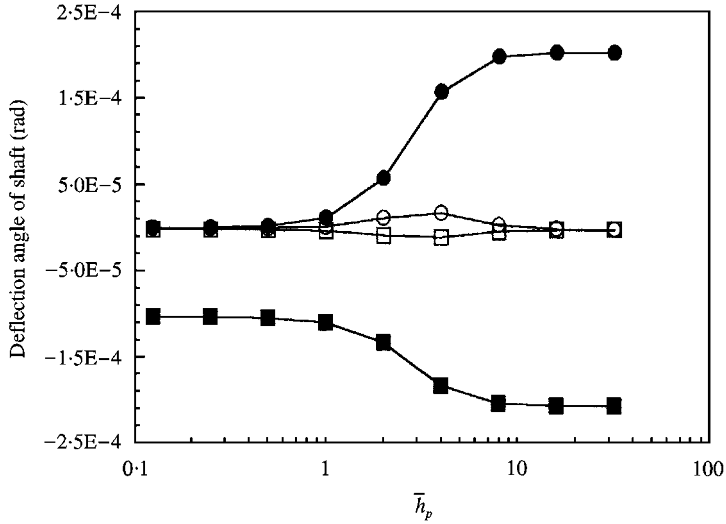

Figure 9. Variations of static deflection angles at both ends versus film thickness. —○— φ_1; —□— φ_2; —●— ψ_1; —■— ψ_2.

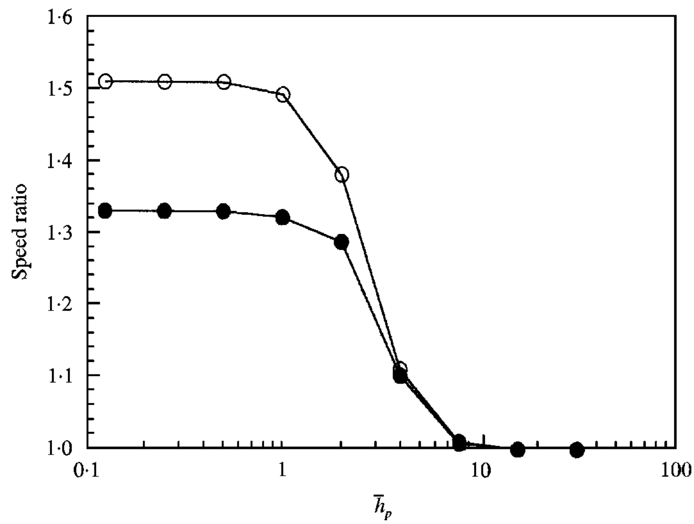

Figure 10. Variations of speed ratios versus film thickness. —○— N^*_{cr}/N_{cr}; —●— N^*_{st}/N_{st}.

limit, the angular displacements at the place where the thrust bearing acts, are eliminated, and the thrust bearing is equivalent to an end face ball bearing.

On the one hand, the axial load that the thrust bearing balances changes the stiffness of the shaft, on the other it changes the film thickness of the thrust bearing. Therefore, it can certainly affect the action of the thrust bearing. Figure 11 shows the variation of the influence of the thrust bearing on the dynamic characteristics of the system versus the axial load. The initial film thickness of the thrust bearing in

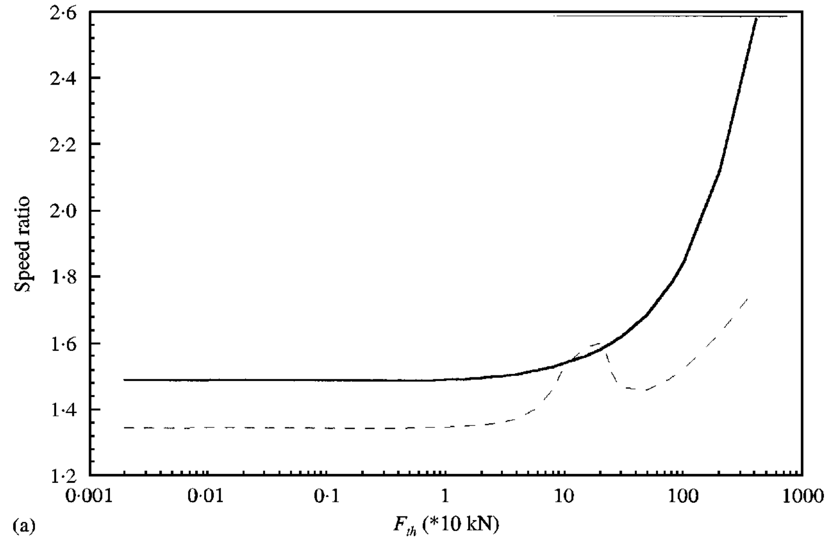

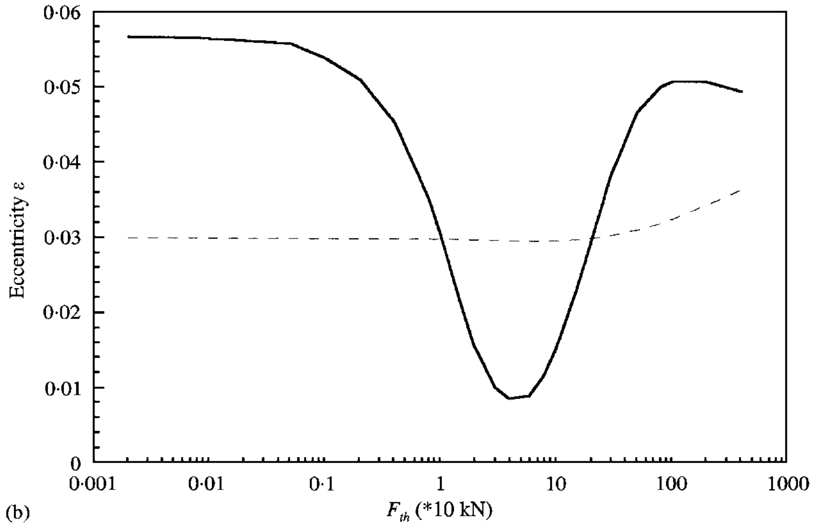

Figure 11. Variation of thrust bearing action versus the axial load. (a) —— N^*_{cr}/N_{cr}, - - - - N^*_{st}/N_{st}; (b) —— LJ; - - - - RJ.

this case is 0·05 mm. The variations of N^*_{cr}/N_{cr} and N^*_{st}/N_{st} are remarkable only when the axial load is very large. It is shown by the figures that N^*_{cr}/N_{cr} varies monotonically, while a fluctuation occurs to N^*_{st}/N_{st}. The fluctuation results from the joint action of the static forces and moments of the thrust bearing. The static forces make the left journal go up, while is more obvious when the axial load is minimum. When the axial load increases to a specific value, as the stiffness of shaft increases, the deflection angles at the thrust bearing decreases, and so does this effect. The static moments, which is related to the static deflection angle, make the left journal go down and the right journal up. As the static loads of journal bearings are not large, the variation of eccentricities shows little effect on the first critical speed, but remarkable effect on the stability threshold speed.

It must be pointed out that the aim here is to investigate the variations of the effect of thrust bearing versus the continuous variation of parameters. Therefore, the parameters may be beyond some restraints, for instance, the film thickness of thrust bearing may be smaller than the allowable minimum thickness, the axial pulling force may exceed the allowable value, and the axial pressing force may exceed the static buckling threshold.

6.2. STIFFNESS OF SHAFT AND STATIC LOAD OF JOURNAL BEARING

Neglecting the mass of the shaft and considering its stiffness only, and by changing the shaft diameter, variable shaft stiffness is obtained. The static loads of journal bearings are changed by exerting similar static forces on both journals. The results for the rotor-bearing system shown in Figure 8 when the oil-film thickness of the thrust bearing is 0·05 mm are given in Figure 12. In this case, the effect of thrust bearing on the first critical speed varies a little; the stiffer and shaft, the weaker the influence of thrust bearing on the first critical speed. The effect of thrust bearing on a flexible rotor varies significantly with the static load on journals. When the static load is large, the thrust bearing may decrease the stability threshold speed of a flexible rotor, which results from the static action of the thrust bearing. The static moments of the thrust bearing are related to the static deflection angles. The more flexible the shaft, the larger the deflection angles at the thrust bearing and the moments of thrust bearing with the result that the static action of the thrust bearing is more significant. When the journals are subjected to medium and large static loads, the variation of the action of thrust bearing on the system versus the shaft stiffness displays a trend of going from small to maximum and from maximum to small. When the static loads are small the variation is monotonic. The above complex variation results from the static action of the thrust bearing. The results shown in Table 4 indicate that the smaller the stiffness and the static forces on journals, the more significant the static action of thrust bearing on the rotor.

6.3. POSITION OF LUMPED MASS

The position of lumped mass shows great effect upon either simply supported rotors or journal-bearing-supported rotors. As it can affect the static and the dynamic deflection simultaneously, it also influences the action of the thrust bearing on rotor systems. Figure 13 shows the variations of speed ratios versus the position of lumped mass. The parameters, except the position of lumped mass, are similar to those used in axial force effect analysis. It can be seen from the figure that when the lumped mass is near the thrust bearing, the change of thrust bearing action is significant. When the lumped mass is far from the thrust bearing, the effect of thrust bearing on the system is weak and changes smoothly with the position of lumped mass. The variation of stability threshold speed ratio versus the position of lumped mass is not monotonic. Comparison between Figures 13(a) and (b) shows that the change of deflection state due to the action of the thrust bearing leads to the changes of the static moments of the thrust bearing which affect the static

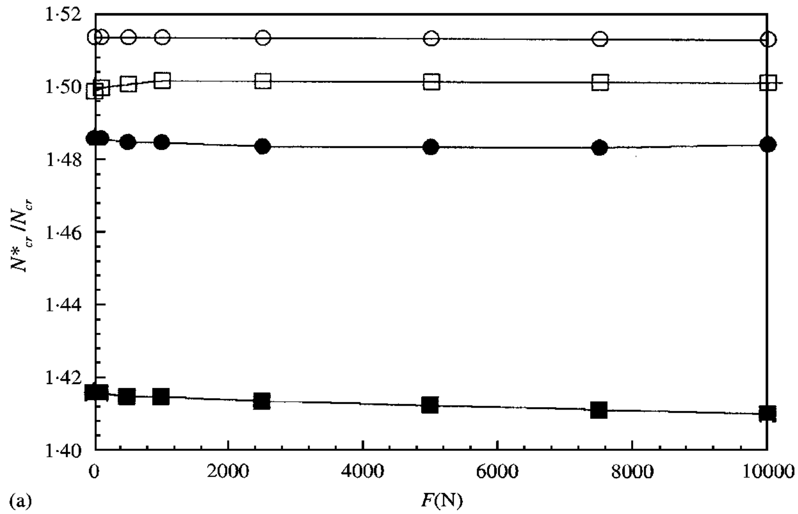

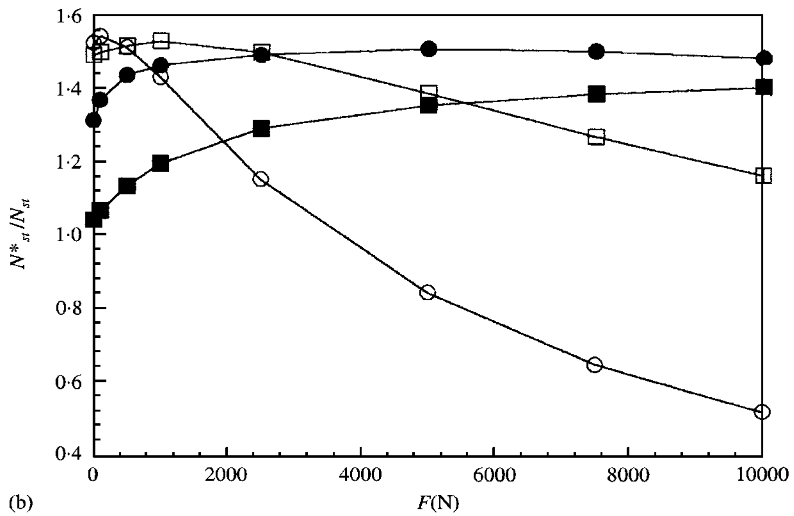

Figure 12. Influences of shaft stiffness and static loads of journal bearings on the effect of thrust bearing. —○— $D = 12{\cdot}5$; —□— $D = 25{\cdot}0$; —●— $D = 50{\cdot}0$; —■— $D = 100{\cdot}0$.

TABLE 4

Eccentricities of both journal bearings at 1000 r/min

D (mm)	F (N)	Thrust bearing	LJ	RJ
100	0	NT	0·86459E − 1	0·86459E − 1
100	0	T	0·93695E − 1	0·79254E − 1
100	10 000	NT	0·79756	0·79756
100	10 000	T	0·79779	0·79733
25	0	NT	0·86459E − 1	0·86459E − 1
25	0	T	0·11681	0·55016E − 1
25	10 000	NT	0·79744	0·79744
25	10 000	T	0·79795	0·79694

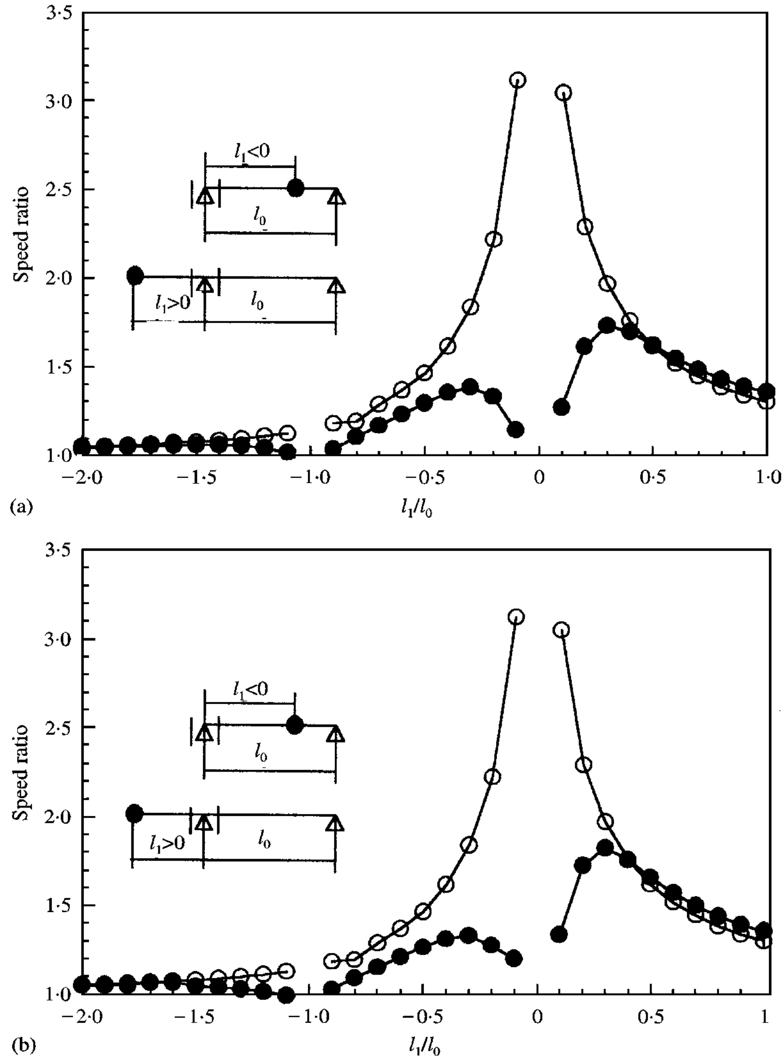

Figure 13. Variation of the thrust bearing action versus the position of lumped mass: (a) considering the static effect; (b) not considering the static effect. —○— N^*_{cr}/N_{cr}; —●— N^*_{st}/N_{st}.

journal positions, and results in the difference of the influence of lumped mass position on the stability threshold speed ratio.

6.4. POSITION OF THRUST BEARING

If the effect of the thrust bearing on vibration modes is neglected, and from the point of view of dynamics only, the action of the thrust bearing is related to the deflection angles where the thrust bearing acts. The larger the deflection angles, the stronger the action. Therefore, for a symmetric rotor system, the action is the strongest when the thrust bearing is positioned at either end of the shaft, and it does not take effect when the thrust bearing is at the disk. But when the static effect of the thrust bearing and the change of vibration modes are considered, the results are different. From Figure 14(a), the maximum action of the thrust bearing is not at the left end, but a certain distance from the left end. At the disk, as the deflection

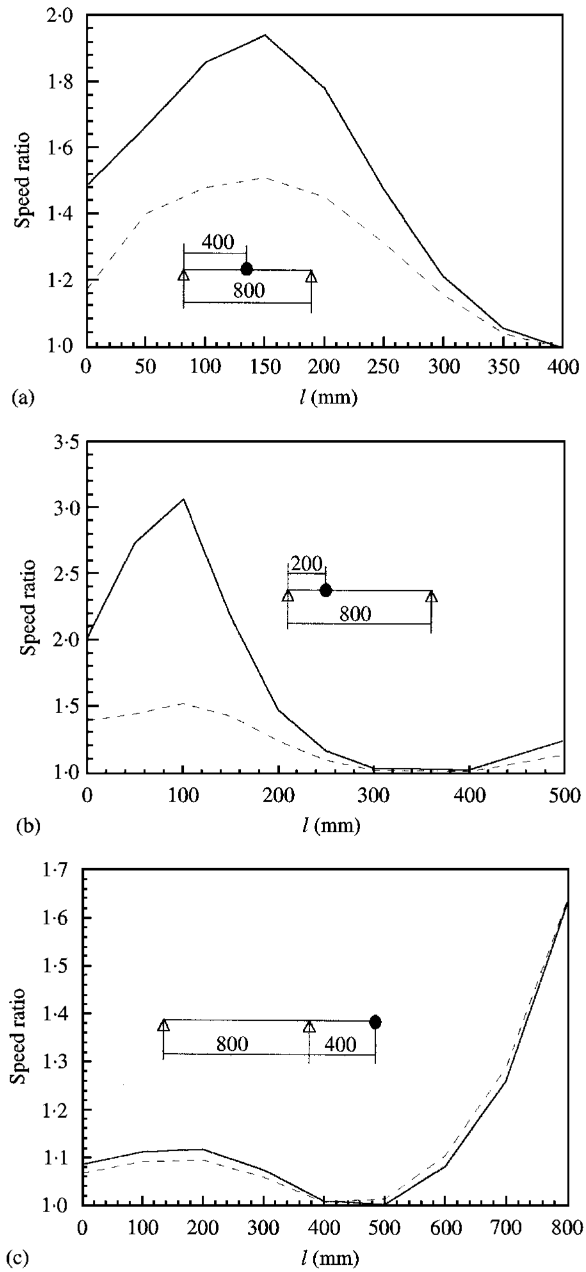

Figure 14. Variation of the thrust bearing action versus the position of lumped mass. (a) —— N^*_{cr}/N_{cr}, - - - - N^*_{st}/N_{st}; (b) —— N^*_{cr}/N_{cr}, - - - - N^*_{st}/N_{st}; (c) —— N^*_{cr}/N_{cr}, - - - - N^*_{st}/N_{st}; (d) —— LJ; - - - - RJ; (e) —— N^*_{cr}/N_{cr}, - - - - N^*_{st}/N_{st}.

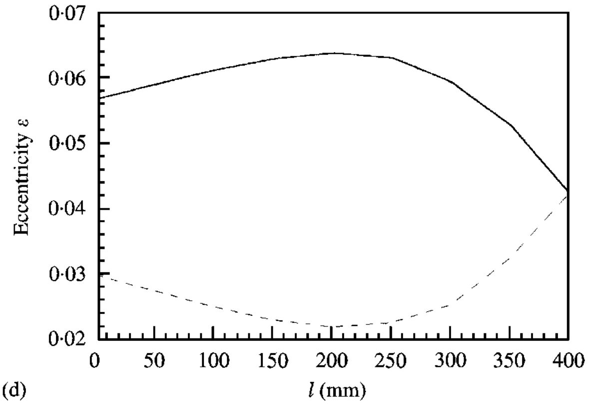

(d)

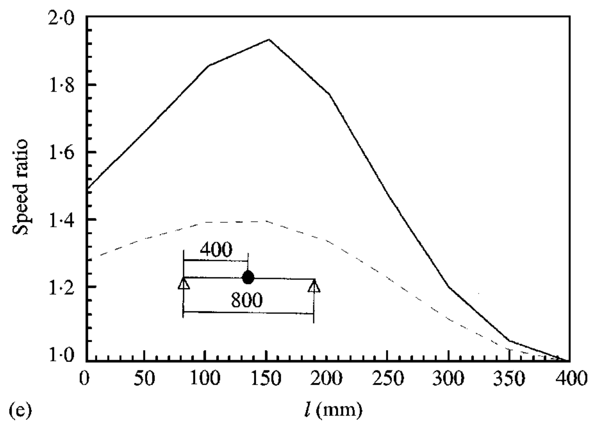

(e)

Figure 14. Continued.

angles are zero, the thrust bearing shows no effect upon the statics and dynamics of the system. Figure 14(d) gives the variations of eccentricities versus the position of thrust bearing at 3000 r/min. The maximum action of the thrust bearing on the statics is not at the left end, but about 200 mm from the left. Figure 14(e) shows the effect of the thrust bearing on the system dynamics when the static action of the thrust bearing is neglected. Comparison between Figures 14(a) and (e) shows the static action is considerable.

The effect of the thrust bearing on another two types of rotors, namely asymmetric rotor and cantilever rotor, are shown in Figures 14(b) and (c) respectively.

6.5. ARRANGEMENT OF THRUST BEARINGS

All the thrust bearings analysed above are double-facet thrust bearings. In this section, two other types of thrust bearing arrangements are discussed. For these two types of arrangements the expansion or contraction of the shaft due to axial force is of the same order as the oil-film thickness of the thrust bearing, and therefore the axial deformation can certainly change the film thickness of thrust bearings. This effect must be accounted for in the static equilibrium equations.

The axial deformation co-ordination condition is

for arrangement (b),

$$h_1 + h_2 = h_{10} + h_{20} + \Delta l, \tag{41}$$

for arrangement (c),

$$h_1 + h_2 = h_{10} + h_{20} - \Delta l. \tag{42}$$

The deformation is

$$\Delta l = \sum_j \frac{T_j l_j}{EA_j}, \tag{43}$$

where T_j is the pulling force, and A_j is the section area.

An iterative procedure based on the proposed in section 4 is applied to solve the static equilibrium equations considering the static axial deformation. The results are listed in Table 5, where the static characteristics are those at 3000 r/min.

From the table, because of the axial deformation, the film thickness of the thrust bearing in (b) and (c) is greater than that in (a), especially when the initial thickness is small. Nevertheless, when the initial film thickness is small, the first critical speeds in (b) and (c) are larger than those in (a), which results from the increase in degrees of freedom restrained by the thrust bearings.

As the lateral forces produced by the thrust bearings in (b) make the journals go up, and the eccentricities of both journal bearings decrease, the stability threshold speed of (b) is lower than that in (c). But when the film thickness of cases (a) and (b) is larger than that of (a), the stability threshold speeds are lower than that of (a). (see Figure 15).

7. CONCLUSION

The model proposed in this paper to investigate the coupled dynamics of a rotor-bearing system equipped with a hydrodynamic thrust bearing can readily take into account such effects as axial force, static coupling and offset-load in journal bearings, etc. The formulation is not only suitable for single-disk rotors which are used as study objects in this paper, but also for multi-disk multi-journal-bearing rotor systems. The investigation has revealed the nature of the action of thrust bearings sufficiently, i.e. thrust bearings couple with the system in statics and dynamics. They not only provide stiffness and damping in a dynamic state, but also change the static deflection of a shaft, and thereby influence the load-sharing of journal bearings in a static state. Therefore, all the parameters influencing the vibration modes and static deflection mode can affect the action of thrust bearings. This effect promotes the use of thrust bearings as a measures to alter the dynamic properties of a machine. It also helps to explain the change in dynamic properties of some machines due to the introduction of thrust bearings.

TABLE 5

Infuence of thrust bearin arrangement on the actions of thrust bearing

$\bar{h}_p$	Arrange-ment	N^*_{cr}/N_{cr}	N^*_{st}/N_{st}	ε_1	ε_2	$\bar{h}_1$	φ_1	φ_2	ψ_1	ψ_2
3·0	(a)	1·2152	1·1918	0·339E − 1	0·247E − 1	3·0	0·156E − 4	− 0·825E − 5	0·891E − 4	− 0·122E − 3
3·0	(b)	1·2109	1·1242	0·115E − 1	0·115E − 1	3·158	0·146E − 4	− 0·146E − 4	0·105E − 4	− 0·105E − 3
3·0	(c)	1·2064	1·1871	0·684E − 1	0·684E − 1	3·158	0·147E − 4	0·147E − 4	0·106E − 3	− 0·106E − 3
1·0	(a)	1·5125	1·3224	0·395E − 1	0·190E − 1	1·0	0·164E − 5	− 0·185E − 5	0·956E − 5	− 0·822E − 4
1·0	(b)	1·5918	1·2363	0·304E − 1	0·304E − 1	1·653	0·758E − 5	− 0·758E − 5	0·373E − 4	− 0·373E − 4
1·0	(c)	1·5900	1·3573	0·865E − 1	0·865E − 1	1·653	0·764E − 5	− 0·764E − 5	0·375E − 1	− 0·375E − 1
0·1	(a)	1·4864	1·3145	0·402E − 1	0·183E − 1	0·1	0·900E − 8	− 0·109E − 5	0·126E − 6	− 0·774E − 4
0·1	(b)	1·7180	1·2319	0·270E − 1	0·270E − 1	1·242	0·383E − 5	− 0·383E − 5	0·201E − 4	− 0·201E − 4
0·1	(c)	1·1717	1·4050	0·834E − 1	0·834E − 1	1·242	0·387E − 5	− 0·387E − 5	0·203E − 4	− 0·203E − 4

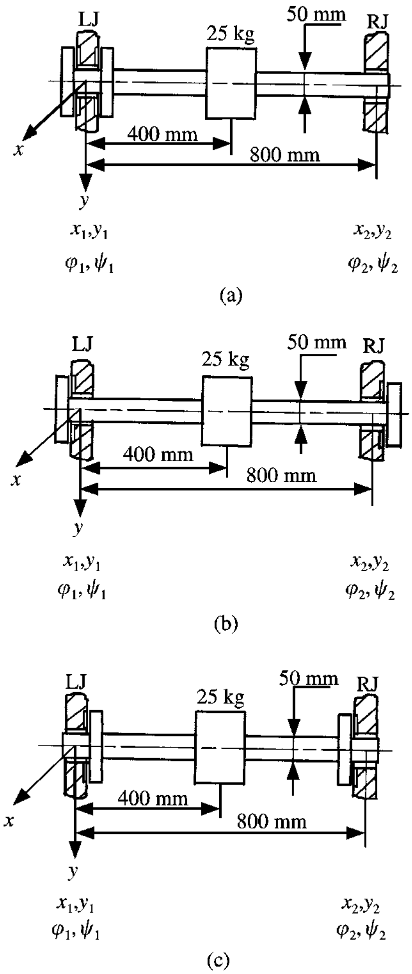

Figure 15. Three arrangement types of thrust bearings.

ACKNOWLEDGMENTS

The authors are grateful for the financial supports from Natural Science Foundation of China (Grant No. 59493700) and Ministry of Science and Technology of China (Grant No. PD9521902).

REFERENCES

1. H. H. JEFFCOTT 1919 *Philosophical Magazine* **37**. The lateral vibration of loaded shafts in the neighborhood of a whirling speed: the effect of want of balance.
2. A. M. KIMBAL 1924 *General Electrical Review* **27**, 244–251. Internal friction theory of shaft whipping.
3. B. L. NEWKIRK and H. D. TAYLOR 1925 *General Electrical Review* **28**, 559. Shaft whipping due to oil action in journal bearings.

4. J. S. ALFORD 1965 *Transactions of ASME, Journal of Engineering for Power* **87**, 333–334. Protecting turbomachinery from self-excited rotor whirl.
5. J. GLIENICKE 1996 *Dissertation TH Karlsruhe*. Feder und Dampflungskonstanten von Gleitlagern fur Turbomaschinen unde dern Einfluss auf das Schwingungsverhalten eines einfachen Rotors.
6. J. W. LUND 1974 *Transactions ASME, Journal of Engineering for Industry* **92**, 509–517. Stability and damped critical speeds of a flexible rotor in fluid-film bearings
7. R. GASCH 1976 *The 1st International Conference on Vibration in Rotating Machinery*, University of Cambridge, 123–128. Dynamic behavior of a simple rotor with a cross sectional crack.
8. R. H. BANNISTER 1980 *Transactions of ASME, Journal of Mechanical Design* **102**, 130–139. Method for modelling flanged and curved couplings for dynamic analysis of complex rotor construction.
9. C. J. MYERS 1984 *Transactions of ASME, Journal of Applied Mechanics* **51**, 244–250. Bifurcation theory applied to oil whirl in plain cylindrical journal bearings.
10. P. HOLLIS and D. L. TAYLOR 1986 *Transactions of ASME Journal of Tribology* **108**, 184–189. Hopf bifurcation to limit cycles in fluid film bearings.
11. P. S. KEOGH and C. R. BURROWS 1995 *Proceedings ImechE:C* **209**, 155–168. Optimization of vibration controllers for steady and transient excitation of flexible rotors.
12. T. SOMEYA 1989 *Journal-Bearing Data Book*. Berlin Springer.
13. I. ETSION 1978 *Transactions ASME Journal of Lubrication Technology* **100**, 279–286. Design charts for arbitrarily pivoted liquid-lubricated flat-sector-pad thrust bearings.
14. M. C. JENG and A. Z. SZERI 1986 *Transactions ASME Journal of Tribology* **108**, 195–218. A thermodynamic solution of pivoted thrust pads.
15. Q. ZHU, Y. B. XIE and L. YU 1990 *Proceedings IC-HBRSD, Xi'an*, 219–224. Axial transient forces of thrust bearing rotor system in a turboexpander.
16. N. MITTWOLLEN, T. HEGEL and J. GLIENICKE 1991 *Transactions ASME Journal of Tribology* **113**, 811–818. Effect of hydrodynamic thrust bearings on lateral shaft vibrations.
17. W. D. MARSCHER 1986 *Radial Loads and Axial Thrusts on Centrifugal Pumps* 17–38. The effect of fluid forces at various operation conditions on the vibrations of vertical pumps.
18. W. BOGUSZ *et al.* 1992 *Vibrations and waves: Part A Vibrations*, 175–176. Amsterdam: Elsevier.
19. T. S. ZHENG, W. M. LIU and Z. B. CAI 1989 *Computers and Structures* **33**, 1139–1143. A generalized inverse iteration method for solution of quadratic eigenvalue problems in structural dynamic analysis.

APPENDIX A: NOMENCLATURE

A	section area
B	width of pad
D_0	diameter of journal bearing
E	elastic module
F_{th}	external load in the axial direction
L	length of journal bearing
M, N	moment
M_k, N_k	external moments
M_x^p, M_y^p, M_z^p	moment due to normal oil-film pressure
N_{cr}	critical speed
N_{st}	stability threshold speed

P_g	weight of lumped mass
S	lateral force
T	axial force
W_x, W_y, W_z	forces due to normal oil-film pressure
$[M], [C], [K]$	mass, damping and stiffness matrices
$\sum P$	external lateral force
d	damping
h	oil-film thickness
h_p	oil-film thickness on pitch line
h_e	reference oil-film thickness
k	stiffness
l	length
m	mass
p	normal oil-film pressure
r	radial co-ordinate of point
t	time
x, y, z	Cartesian co-ordinates
$\mathbf{i}, \mathbf{j}, \mathbf{k}$	base vectors of Cartesian co-ordinates
Ψ	clearance ratio of journal bearing
Ω_j	domain of integration
α_0	wedge angle of pad
α_j	angular position of the jth pad
φ, ψ	tilting angles
μ	dynamic viscosity of oil
θ	angular co-ordinate of point
θ_p	angular position of pitch line
$\theta_x, \theta_y, \theta_z$	moments of inertia

Subscripts

j	pad j, shaft element j
0	static

Superscripts

M	moment
W	force
R	right hand
$\bar{}$	dimensionless variable
$\dot{}$	derivative with time
$\tilde{}$	variable in local co-ordinate system

APPENDIX B: DERIVATIONS OF MATRIX $[A_3]_j$

From Figure 2,

$$W_{xj} = \tilde{W}_{xj}\cos\alpha_j + \tilde{W}_{yj}\sin\alpha_j,\ W_{yj} = -\tilde{W}_{xj}\sin\alpha_j + \tilde{W}_{yj}\cos\alpha_j, \tag{B.1}$$

$$\psi = \psi_j\cos\alpha_j - \varphi_j\sin\alpha_j,\ \varphi = \psi_j\sin\alpha_j + \varphi_j\cos\alpha_j, \tag{B.2}$$

therefore,

$$
\begin{aligned}
\Delta W_{xj} = {} & (\tilde{k}^{W}_{xhj}\Delta h_p + \tilde{k}^{W}_{x\psi j}\Delta\psi_j + \tilde{k}^{W}_{x\varphi j}\Delta\varphi_j)\cos\alpha_j \\
& + (\tilde{k}^{W}_{yhj}\Delta h_p + \tilde{k}^{W}_{y\psi j}\Delta\psi_j + \tilde{k}^{W}_{y\varphi j}\Delta\varphi_j)\sin\alpha_j \\
& + (\tilde{d}^{W}_{xhj}\dot{h}_p + \tilde{d}^{W}_{x\psi j}\dot{\psi}_j + \tilde{d}^{W}_{x\varphi j}\dot{\varphi}_j)\cos\alpha_j \\
& + (\tilde{d}^{W}_{yhj}\dot{h}_p + \tilde{d}^{W}_{y\psi j}\dot{\psi}_j + \tilde{d}^{W}_{y\varphi j}\dot{\varphi}_j)\sin\alpha_j \\
= {} & [\tilde{k}^{W}_{xhj}\Delta h_p + \tilde{k}^{W}_{x\psi j}(\Delta\psi\cos\alpha_j + \Delta\varphi\sin\alpha_j) \\
& + \tilde{k}^{W}_{x\varphi j}(-\Delta\psi\sin\alpha_j + \Delta\varphi\cos\alpha_j)]\cos\alpha_j \\
& + [\tilde{k}^{W}_{yhj}\Delta h_p + \tilde{k}^{W}_{y\psi j}(\Delta\psi\cos\alpha_j + \Delta\varphi\sin\alpha_j) \\
& + \tilde{k}^{W}_{y\varphi j}(-\Delta\psi\sin\alpha_j + \Delta\varphi\cos\alpha_j)]\sin\alpha_j \\
& + [\tilde{d}^{W}_{xhj}\dot{h}_p + \tilde{d}^{W}_{x\psi j}(\dot{\psi}\cos\alpha_j + \dot{\varphi}\sin\alpha_j) \\
& + \tilde{d}^{W}_{x\varphi j}(-\dot{\psi}\sin\alpha_j + \dot{\varphi}\cos\alpha_j)]\cos\alpha_j \\
& + [\tilde{d}^{W}_{yhj}\dot{h}_p + \tilde{d}^{W}_{y\psi j}(\dot{\psi}\cos\alpha_j + \dot{\varphi}\sin\alpha_j) \\
& + \tilde{d}^{W}_{y\varphi j}(-\dot{\psi}\sin\alpha_j + \dot{\varphi}\cos\alpha_j)]\sin\alpha_j \\
= {} & (\tilde{k}^{W}_{xhj}\cos\alpha_j + \tilde{k}^{W}_{yhj}\sin\alpha_j)\Delta h_p \\
& + (\tilde{k}^{W}_{x\psi j}\cos^2\alpha_j - \tilde{k}^{W}_{x\varphi j}\sin\alpha_j\cos\alpha_j + \tilde{k}^{W}_{y\psi j}\sin\alpha_j\cos\alpha_j - \tilde{k}^{W}_{y\varphi j}\sin^2\alpha_j)\Delta\psi \\
& + (\tilde{k}^{W}_{x\psi j}\sin\alpha_j\cos\alpha_j + \tilde{k}^{W}_{x\varphi j}\cos^2\alpha_j + \tilde{k}^{W}_{y\psi j}\sin^2\alpha_j + \tilde{k}^{W}_{y\varphi j}\cos\alpha_j\sin\alpha_j)\Delta\varphi \\
& + (\tilde{d}^{W}_{xhj}\cos\alpha_j + \tilde{d}^{W}_{yhj}\sin\alpha_j)\dot{h}_p \\
& + (\tilde{d}^{W}_{x\psi j}\cos^2\alpha_j - \tilde{d}^{W}_{x\varphi j}\sin\alpha_j\cos\alpha_j + \tilde{d}^{W}_{y\psi j}\cos\alpha_j\sin\alpha_j - \tilde{d}^{W}_{y\varphi j}\sin^2\alpha_j)\dot{\psi} \\
& + (\tilde{d}^{W}_{x\psi j}\sin\alpha_j\cos\alpha_j + \tilde{d}^{W}_{x\varphi j}\cos^2\alpha_j + \tilde{d}^{W}_{y\psi j}\sin^2\alpha_j + \tilde{d}^{W}_{y\varphi j}\cos\alpha_j\sin\alpha_j)\dot{\varphi};
\end{aligned}
\tag{B.3}
$$

$$
\begin{aligned}
\Delta W_{yj} = & -(\tilde{k}^W_{xhj}\Delta h_p + \tilde{k}^W_{x\psi j}\Delta\psi_j + \tilde{k}^W_{x\varphi j}\Delta\varphi_j)\sin\alpha_j \\
& + (\tilde{k}^W_{yhj}\Delta h_p + \tilde{k}^W_{y\psi j}\Delta\psi_j + \tilde{k}^W_{y\varphi j}\Delta\varphi_j)\cos\alpha_j \\
& - (\tilde{d}^W_{xhj}\dot{h} + \tilde{d}^W_{x\psi j}\dot{\psi}_j + \tilde{d}^W_{x\varphi j}\dot{\varphi}_j)\sin\alpha_j + (\tilde{d}^W_{xhj}\dot{h}_p + \tilde{d}^W_{y\psi j}\dot{\psi}_j + \tilde{d}^W_{y\varphi j}\dot{\varphi}_j)\cos\alpha_j \\
= & -[\tilde{k}^W_{xhj}\Delta h_p + \tilde{k}^W_{x\psi j}(\Delta\psi\cos\alpha_j + \Delta\varphi\sin\alpha_j) \\
& + \tilde{k}^W_{x\varphi j}(-\Delta\psi\sin\alpha_j + \Delta\varphi\cos\alpha_j)]\sin\alpha_j \\
& + [\tilde{k}^W_{yhj}\Delta h_p + \tilde{k}^W_{y\psi j}(\Delta\psi\cos\alpha_j + \Delta\varphi\sin\alpha_j) \\
& + \tilde{k}^W_{y\varphi j}(-\Delta\psi\sin\alpha_j + \Delta\varphi\cos\alpha_j)]\cos\alpha_j \\
& - [\tilde{d}^W_{xhj}\dot{h}_p + \tilde{d}^W_{x\psi j}(\dot{\psi}\cos\alpha_j + \dot{\varphi}\sin\alpha_j) \\
& + \tilde{d}^W_{x\varphi j}(-\dot{\psi}\sin\alpha_j + \dot{\varphi}\cos\alpha_j)]\sin\alpha_j \\
& + [\tilde{d}^W_{yhj}\dot{h}_p + \tilde{d}^W_{y\psi j}(\dot{\psi}\cos\alpha_j + \dot{\varphi}\sin\alpha_j) \\
& + \tilde{d}^W_{y\varphi j}(-\dot{\psi}\sin\alpha_j + \dot{\varphi}\cos\alpha_j)]\cos\alpha_j \\
= & (-\tilde{k}^W_{xhj}\sin\alpha_j + \tilde{k}^W_{yhj}\cos\alpha_j)\Delta h_p \\
& + (-\tilde{k}^W_{x\psi j}\sin\alpha_j\cos\alpha_j + \tilde{k}^W_{x\varphi j}\sin^2\alpha_j + \tilde{k}^W_{y\psi j}\cos^2\alpha_j \\
& - \tilde{k}^W_{y\varphi j}\sin\alpha_j\cos\alpha_j)\Delta\psi \\
& + (-\tilde{k}^W_{x\psi j}\sin^2\alpha_j - \tilde{k}^W_{x\varphi j}\sin\alpha_j\cos\alpha_j + \tilde{k}^W_{y\psi j}\sin\alpha_j\cos\alpha_j + \tilde{k}^W_{y\varphi j}\cos^2\alpha_j)\Delta\varphi \\
& + (-\tilde{d}^W_{xhj}\sin\alpha_j + \tilde{d}^W_{yhj}\cos\alpha_j)\dot{h}_p \\
& + (-\tilde{d}^W_{x\psi j}\sin\alpha_j\cos\alpha_j + \tilde{d}^W_{x\varphi j}\sin^2\alpha_j + \tilde{d}^W_{y\psi j}\cos^2\alpha_j \\
& - \tilde{d}^W_{y\varphi j}\sin\alpha_j\cos\alpha_j)\dot{\psi} \\
& + (-\tilde{d}^W_{x\psi j}\sin^2\alpha_j - \tilde{d}^W_{x\varphi j}\sin\alpha_j\cos\alpha_j + \tilde{d}^W_{y\psi j}\sin\alpha_j\cos\alpha_j \\
& + \tilde{d}^W_{y\varphi j}\cos^2\alpha_j)\dot{\varphi} \qquad \text{(B4)}
\end{aligned}
$$

Matrix $[A_3]_j$ can be obtained from the above two equations.

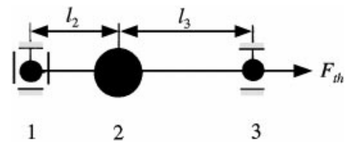

Figure 16. Lumped mass model of a rotor-bearing system with a hydrodynamic thrust bearing.

APPENDIX C: DETAILED FORM OF EQUATION (25)

The system motion equations for a rotor-bearing system which is simplified into a three-lumped-mass model shown in Figure 16 are

$$
\begin{bmatrix}
m_1 &&&&&&&&&&&& \\
& m_1 &&&&&&&&&&& \\
&& \theta_{x1} &&&&&&&&&& \\
&&& \theta_{y1} &&&&&&&&& \\
&&&& m_2 &&&&&&&& \\
&&&&& m_2 &&&&&&& \\
&&&&&& \theta_{x2} &&&&&& \\
&&&&&&& \theta_{x2} &&&&& \\
&&&&&&&& m_3 &&&& \\
&&&&&&&&& m_3 &&& \\
&&&&&&&&&& \theta_{x3} && \\
&&&&&&&&&&& \theta_{x3} & \\
&&&&&&&&&&&& m_1+m_2+m_3
\end{bmatrix}
\begin{Bmatrix}
\ddot{x}_1 \\ \ddot{y}_1 \\ \ddot{\varphi}_1 \\ \ddot{\psi}_1 \\ \ddot{x}_2 \\ \ddot{y}_2 \\ \ddot{\varphi}_2 \\ \ddot{\psi}_2 \\ \ddot{x}_3 \\ \ddot{y}_3 \\ \ddot{\varphi}_3 \\ \ddot{\psi}_3 \\ \ddot{h}_p
\end{Bmatrix}
$$

$$
+\begin{bmatrix}
d_{xx1} & d_{xy1} & -d^W_{x\varphi} & -d^W_{x\psi} &&&&&&&&& -k^W_{x\varphi} \\
d_{yx1} & d_{yy1} & -d^W_{y\varphi} & -d^W_{y\psi} &&&&&&&&& -k^W_{y\varphi} \\
0 & -\omega\theta_{z1} & -d^M_{y\varphi} & -d^M_{y\psi} &&&&&&&&& -k^M_{y\varphi} \\
\omega\theta_{z1} & 0 & d^M_{x\varphi} & d^M_{x\psi} &&&&&&&&& k^M_{x\varphi} \\
&&&& 0 & 0 & 0 & 0 &&&&& 0 \\
&&&& 0 & 0 & 0 & 0 &&&&& 0 \\
&&&& 0 & -\omega\theta_{z2} & 0 & 0 &&&&& 0 \\
&&&& \omega\theta_{z2} & 0 & 0 & 0 &&&&& 0 \\
&&&&&&&& d_{xx2} & d_{xyz} & 0 & 0 & 0 \\
&&&&&&&& d_{yx2} & d_{yy2} & 0 & 0 & 0 \\
&&&&&&&& 0 & -\omega\theta_{z3} & 0 & 0 & 0 \\
&&&&&&&& \omega\theta_{z3} & 0 & 0 & 0 & 0 \\
0 & 0 & -d^W_{z\varphi} & -k^W_{z\psi} & 0 & 0 & 0 & 0 & 0 & 0 & 0 & 0 & -k^W_{zh}
\end{bmatrix}
\begin{Bmatrix}
\dot{x}_1 \\ \dot{y}_1 \\ \dot{\varphi}_1 \\ \dot{\psi}_1 \\ \dot{x}_2 \\ \dot{y}_2 \\ \dot{\varphi}_2 \\ \dot{\psi}_2 \\ \dot{x}_3 \\ \dot{y}_3 \\ \dot{\varphi}_3 \\ \dot{\psi}_3 \\ \dot{h}_p
\end{Bmatrix}
$$

$$\left[\begin{array}{ccccccccccccc}
\frac{12EI_2}{l_2^3}+k_{xx1} & k_{xy1} & \frac{6EI_2}{l_2^2}-k^W_{x\varphi} & -k^W_{x\psi} & -\frac{12EI_2}{l_2^3} & 0 & \frac{6EI_2}{l_2^2}-F_{th} & 0 & 0 & 0 & 0 & 0 & -k^W_{xh} \\
k_{yx1} & \frac{12EI_2}{l_2^3}+k_{yy1} & -k^W_{y\varphi} & \frac{6EI_2}{l_2^2}-k^W_{y\psi} & 0 & -\frac{12EI_2}{l_2^3} & 0 & \frac{6EI_2}{l_2^2}-F_{th} & 0 & 0 & 0 & 0 & -k^W_{xh} \\
\frac{6EI_2}{l_2^2}-F_{th} & 0 & \frac{4EI_2}{l_2}-k^M_{y\varphi} & -k^M_{y\psi} & -\frac{6EI_2}{l_2^2}+F_{th} & 0 & \frac{2EI_2}{l_2}-F_{th}l_2 & & 0 & 0 & 0 & 0 & -k^M_{yh} \\
0 & \frac{6EI_2}{l_2^2}-F_{th} & k^M_{x\varphi} & \frac{4EI_2}{l_2}+k^M_{x\psi} & 0 & -\frac{6EI_2}{l_2}+F_{th} & 0 & \frac{2EI_2}{l_2}-F_{th}l_2 & 0 & 0 & 0 & 0 & k^M_{xh} \\
-\frac{12EI_2}{l_2^3} & 0 & -\frac{6EI_2}{l_2^2} & 0 & \frac{12EI_2}{l_2^3}+\frac{12EI_3}{l_3^3} & 0 & \frac{6EI_3}{l_3^2}-\frac{6EI_2}{l_2^2}+F_{th} & 0 & -\frac{12EI_3}{l_3^3} & 0 & \frac{6EI_3}{l_3^2}-F_{th} & 0 & 0 \\
0 & -\frac{12EI_2}{l_2^3} & 0 & -\frac{6EI_2}{l_2^3} & 0 & \frac{12EI_2}{l_2^3}+\frac{12EI_3}{l_3^3} & 0 & \frac{6EI_3}{l_3^2}-\frac{6EI_2}{l_2^2}+F_{th} & 0 & -\frac{12EI_3}{l_3^3} & 0 & \frac{6EI_3}{l_3^2}-F_{th} & 0 \\
\frac{6EI_2}{l_2^2} & 0 & \frac{1}{a_1}\left[\left(\frac{2EI_2}{l_2}-F_{th}l_2\right)+F_{th}\left(l_2+\frac{F_{th}l_2^3}{6EI_2}\right)\right] & 0 & \frac{6EI_3}{l_3^2}-\frac{6EI_2}{l_2^2}-F_{th} & 0 & \frac{4EI_3}{l_3}+\frac{4EI_2}{l_2} & 0 & -\frac{6EI_3}{l_3^2}+F_{th} & 0 & \frac{2EI_3}{l_3}-F_{th}l_3 & 0 & 0 \\
0 & \frac{6EI_2}{l_2^2} & 0 & \frac{1}{a_2}\left[\left(\frac{2EI_2}{l_2}-F_{th}l_2\right)+F_{th}\left(l_2+\frac{F_{th}l_2^3}{6EI_2}\right)\right] & 0 & \frac{6EI_3}{l_3^2}-\frac{6EI_2}{l_2^2}-F_{th} & 0 & \frac{4EI_3}{l_3}+\frac{4EI_2}{l_2} & 0 & -\frac{6EI_3}{l_3^2}+F_{th} & 0 & \frac{2EI_3}{l_3}-F_{th}l_3 & 0 \\
0 & 0 & 0 & 0 & -\frac{12EI_3}{l_3^3} & 0 & -\frac{6EI_3}{l_3^2} & 0 & \frac{12EI_3}{l_3^3}+k_{yy2} & k_{xy2} & -\frac{6EI_3}{l_3^2}+F_{th} & 0 & 0 \\
0 & 0 & 0 & 0 & 0 & -\frac{12EI_3}{l_3^2} & 0 & -\frac{6EI_3}{l_3^2} & k_{yx2} & \frac{12EI_3}{l_3^3}+k_{yy2} & 0 & -\frac{6EI_3}{l_3^2}+F_{th} & 0 \\
0 & 0 & 0 & 0 & \frac{6EI_3}{l_3^2} & 0 & \frac{1}{a_2}\left[\left(\frac{2EI_3}{l_3}-F_{th}l_3\right)+F_{th}\left(l_3+\frac{F_{th}l_3^3}{6EI_3}\right)\right] & 0 & -\frac{6EI_3}{l_3^2} & 0 & \frac{4EI_3}{l_3} & 0 & \\
0 & 0 & 0 & 0 & 0 & \frac{6EI_3}{l_3^2} & 0 & \frac{1}{a_2}\left[\left(\frac{2EI_3}{l_3}-F_{th}l_3\right)+F_{th}\left(l_3+\frac{F_{th}l_3^3}{6EI_3}\right)\right] & 0 & -\frac{6EI_3}{l_3^2} & 0 & \frac{4EI_3}{l_3} & 0 \\
0 & 0 & -k^W_{z\varphi} & -k^W_{z\psi} & 0 & 0 & 0 & & 0 & 0 & 0 & 0 & -k^W_{zh}
\end{array}\right]$$

Contd. from page 871.

$$\times \begin{Bmatrix} x_1 \\ y_1 \\ \varphi_1 \\ \psi_1 \\ x_2 \\ y_2 \\ \varphi_2 \\ \psi_2 \\ x_3 \\ y_3 \\ \varphi_3 \\ \psi_3 \\ h_p \end{Bmatrix} = 0, \tag{C1}$$

where

$$a_1 = 1 + \frac{F_{th}^2 l_2^4}{12(EI_2)^2}, \qquad a_2 = 1 + \frac{F_{th}^2 l_3^4}{12(EI_3)^2}.$$